KTH ROYAL INSTITUTE
OF TECHNOLOGY

Degree Project in Technology

First cycle, 15 credits

Analysis of granulated carbide powder and how it affects pressing

EMMA HJORTZBERG-NORDLUND, LINNÉA LUNDEMO MATTSSON & MAEVA ANFOSSI

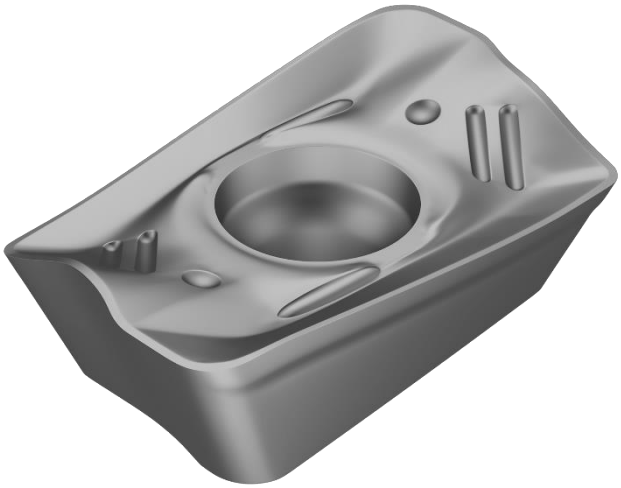

Stockholm, Sweden 2023

Abstract

During the pressing of powder mixtures to make cemented carbide tools, the degree to which the powder spreads to fill the die and to which it compacts is uncertain. This leads to inconsistent dimensions and densities in the finished product. This performance changes with the composition of the powder, including the amount of pressing agent in the mixture, the particle size distribution and particle shape.

One way to quantify the degree to which powder will spread to fill the mold evenly is using the property called 'flowability'. There are several techniques by which flowability can be measured, and each technique does not always give results that are consistent with other techniques. It is, therefore, important to know what technique(s) predict(s) the final behavior of the powder in this application before it is used in quality assurance or to design a process. Additionally, powder size distribution and shape metrics are measured using dynamic image analysis to investigate if there is any relationship between key values of these properties and compaction behavior.

In this study, static Angle of repose, Tap Density, Hall flow time and Powder rheometry were benchmarked against each other and against the dimensions of presses and liquid phase sintered tool inserts to understand which technique had the strongest dependence on the compactability, which was defined as the ratio of the tallest dimension in the insert to the smallest.

After the study, the results showed that a more extensive particle size distribution improves the compaction properties and that the powders with a higher resistance to a rotating blade tend to have better compaction properties. On the other hand, a clear pattern for the results of all measurement methods and the correlation between the compaction behavior of the carbide tools could not be discerned. In conclusion, the study showed that it is possible to determine a relationship between the results of measurement methods and the compaction behavior of powders.

By using simple tests to predict the compactability properties, both money and time can be saved on the research of new, improved powder. Furthermore, the implementation of this study can lead to even better pressing and compactibility properties in the future for cemented carbide tools.

Keywords

Cemented Carbide Tools, Pressing Agent, Flowability, Tap Density, Angle Of Repose, Hall Flow Time, Particle Size Distribution, Powder Rheometer, Compatibility

Sammanfattning

Vid pressning av pulverblandningar för tillverkning av hårdmetallverktyg är det osäkert i vilken grad pulvret sprider sig för att fylla matrisen och i vilken grad det komprimeras. Detta leder till inkonsekventa dimensioner och densiteter i den färdiga produkten. Denna prestanda förändras med pulvrets sammansättning, inklusive mängden bindemedel som finns i blandningen, partikelstorleksfördelningen och partikelformen.

Ett sätt att kvantifiera i vilken grad pulvret sprids för att fylla formen jämnt är att använda den egenskap som kallas "flytbarhet". Det finns flera tekniker för att mäta flytbarhet, och varje teknik ger inte alltid resultat som överensstämmer med andra tekniker. Det är därför viktigt att veta vilken eller vilka tekniker som förutsäger pulvrets slutliga beteende i denna tillämpning innan den används i kvalitetssäkring eller för att utforma en process. Vidare mäts pulvrets partikelstorleksfördelning och form med dynamisk bildanalys för att undersöka om det finns något samband mellan nyckelvärden för dessa egenskaper och komprimeringsbeteendet.

I den här studien jämfördes statisk rasvinkel, tapp densitet, hall flödestid och pulverreometri samt med dimensionerna på pressar och sintrade verktygsinsatser i vätskefas för att förstå vilken teknik som hade det starkaste beroendet på kompatibiliteten, vilket definieras som förhållandet mellan den högsta dimensionen i insatsen och den minsta.

Efter studien visade resultaten att en mer omfattande partikelstorleksfördelning förbättrar komprimeringsegenskaperna och att pulver med högre motståndskraft mot ett roterande blad tenderar att ha bättre komprimeringsegenskaper. Vidare kunde inte ett tydligt mönster för resultaten för alla mätmetoder och sambandet på komprimeringbeteendet för hårmetallverktygen urskiljas. Sammanfattningsvis visade studien på att det går att använda sig av mätmetoder för att kunna urskilja ett samband mellan resultaten på mätmetoderna och pulvers kompaktibillitetsegenskaper.

Genom att använda sig av enkla mätningar för att kunna förutsäga kompaktibilitetsegenskaper samt komprimeringsbeteende kan både pengar respektive tid sparas. Vidare kan genomförandet av denna studie i framtiden leda till ännu bättre pressnings- samt kompaktibilitetsegenskaper för hårdmetallverktyg.

Nyckelord

Hårdmetallverktyg, Pressmedel, Flytbarhet, Tapp Densitet, Rasvinkel, Hall Flödestid, Partikelstorleksfördelning, Pulverrheometri, Kompatibilitet

Table of Contents

1. Introduction **1**
1.1 Sandvik Coromant 1
1.2 Problem 1
1.3 Purpose 1
2. From powders to carbide tools **2**
2.1 Component materials of cemented carbide tool insert precursor 2
2.1.1 Tungsten Carbide-Cobalt 2
2.1.2 Polyethylene Glycol 2
2.1.3 Erucic and Oleic acid 2
2.2 Production of the powder 3
2.3 Compaction and liquid phase sintering 3
2.4 Flowability 3
2.5 Compressibility and Compactibility 4
2.6 Powder Characterisation 4
2.6.1 Hall Flow and Apparent Density 4
2.6.2 Particle Size Distribution 4
2.6.3 The Angle Of Repose 5
2.6.4 Tapped Density 5
2.6.5 Powder Rheometry 5
2.7 Powder Composition 6
3. Method **7**
3.1 Powder Characterisation 7
3.1.1 Hall Flow and Apparent Density 7
3.1.2 Particle Size Distribution 7
3.1.3 Angle Of Repose 8
3.1.4 Tapped Density 8
3.1.5 Powder Rheometry 9
3.2 Measurements of the inserts 9
3.3 Calculation of Errors 10
4. Results **11**
4.1 Powder Characterisation 11
4.1.1 Hall Flow and Apparent Density 11
4.1.2 Particle Size Distribution 13
4.1.3 The Angle Of Repose 17
4.1.4 Tap Density 18
4.1.5 Rheometer FT4 20
4.2 Measurements of the inserts 23
5. Discussion **25**
5.1 Powder Characterisation 25

5.1.1 Correlation between compaction properties and PEG 25
5.1.2 Discussion of the test results 25
5.1.3 Correlation between compressibility and powder tests 27
5.2 Ethical aspects 28
5.3 Sources of Errors 29
6. Conclusions **30**
7. Future Work **31**
8. Acknowledgment **32**
9. References **33**
Appendix: Test values **36**

1. Introduction

1.1 Sandvik Coromant

Sandvik Coromant is a world-leading developer and producer of high-performance manufacturing tools and machining solutions. The company's products are used in metal processing, such as turning, milling and drilling. Sandvik Coromant manufactures both the inserts and the tool holder, the insert being the active piece in cutting metal. The company uses cemented carbide to manufacture the insert.

1.2 Problem

Compaction to complex shapes is difficult and highly dependent on the powder properties such as density and flowability. It is currently difficult to predict how and if the amount and type of pressing agents, Polyethylene Glycol (PEG), will affect the powder's ability to be pressed. Furthermore, there is no clear link between tests on the properties of the powders and their compaction properties.

1.3 Purpose

The aim is to investigate and compare metal powder with different amounts and types of pressing agents using different measurement methods. The purpose will be to link these measurements with the inserts to find a relationship between the powder's properties and the pressing result. The objective is to be able to do more complex shapes during the pressing part with a uniform density throughout the piece, with the intention to better understand the pressing result through powder characterization. The result could further lead to increased pressing performance, but also saving money and time.

2. From powders to carbide tools

2.1 Component materials of cemented carbide tool insert precursor

The powders used in this thesis had all the same composition, fine-grained WC with 10 wt% Co and 0.39 wt% Cr. The difference between the twelve powders is their Polyethylene Glycol (PEG) content. The powders contain both different amounts and different types of PEG. These powders are known to be quite brittle at room temperature. They also have a very high melting temperature, which constrains the manufacturer from using particular processing and testing techniques [1].

2.1.1 Tungsten Carbide-Cobalt

Tungsten Carbide-Cobalt is a composite of hard ceramic Tungsten Carbide particles and ductile metallic Cobalt [2]. Tungsten Carbide-Cobalt has properties including hardness, strength, high malleability and ductility, and good electrical and thermal conductivity [3].

Adding cobalt increases the material's resistance to wear, hardness, and toughness. You can vary the material's properties based on these cobalt contents and the tungsten carbide grain size. The material properties make it suitable for milling, drilling, and pressing tools. Its high strength allows it to break through and drill in other hard materials [4].

Exposure to cobalt can cause eczema, respiratory problems, cardiovascular disease, and cancer [5]. An intake of more than 20 mg of cobalt daily has been shown to cause health problems. The substance can be hazardous by skin contact and inhalation and should therefore be handled carefully. Cobalt is classified as an environmentally hazardous substance and must not be released into the environment or drains [4].

2.1.2 Polyethylene Glycol

PEG is a water-soluble synthetic polymer wax made by adding ethylene oxide to water or ethylene glycol. Its molecular weight ranges from 200-20000 g/mol, and it is soluble in water with low solubility in ethanol [6]. Adding a pressing agent binds the powder particles together so the green body is strong enough to keep its shape until sintering. As PEG has a lower melting temperature than the powder, it will evaporate when the pressed metal is heated during the sintering process. What remains is the metal powder that is pressed and solidified into the desired shape.

2.1.3 Erucic and Oleic acid

Erucic acid is an unsaturated fatty acid. It is a major component present in mustard and rapeseed oils. It is soluble in ethanol and has a density of 0.86 kg/m3. It is mainly used as a lubricant [7].

Oleic acid is also an unsaturated fatty acid. It is abundantly present as the major component of olive oil and many other plant oils. It is miscible with ethanol and has a density of 0.89 kg/m3. It has many uses, the ones interesting in this thesis are as a surfactant and lubricant [8]. The difference of this acid compared to the previous is found in the length of one of the carbon backbone.

2.2 Production of the powder

The raw material is weighed and then put into a ball mill to be milled to the desired particle size. This step is required to achieve the desired properties of the insert. The mill is filled with balls made from tungsten carbide that crush and grind down the material as the mill spins. Milling alcohol is added to the powder, creating a slurry. It is this slurry that the pressing agent, PEG, is added. The next step is spray drying the powder to make it easier for the powder to fill the press cavities. The slurry with the powder is sprayed into a heated chamber, and forms solidified spherical droplets. During the process, the milling alcohol evaporates, and a powder with spherical particles containing only the metals and the PEG is created [9].

2.3 Compaction and liquid phase sintering

A press consists of a die with moving upper and lower punches. As shown in Figure 1, the powder is filled in a die, and the upper punch presses the powder against the lower punch. The result is a solid structure called green body, made of compressed granules. During the pressing, the volume of the powder shrinks by roughly 50 percent. The next step is liquid phase sintering which is a heat treatment of the green body. The heat evaporates the PEG, and the cobalt melts, creating a pore-free solid structure. During the sintering, the green body volume shrinks roughly 50 percent. Shrinkage will be most significant in the parts of the greenbody with the lowest density. It is essential to consider this when calculating the final product's shape [9].

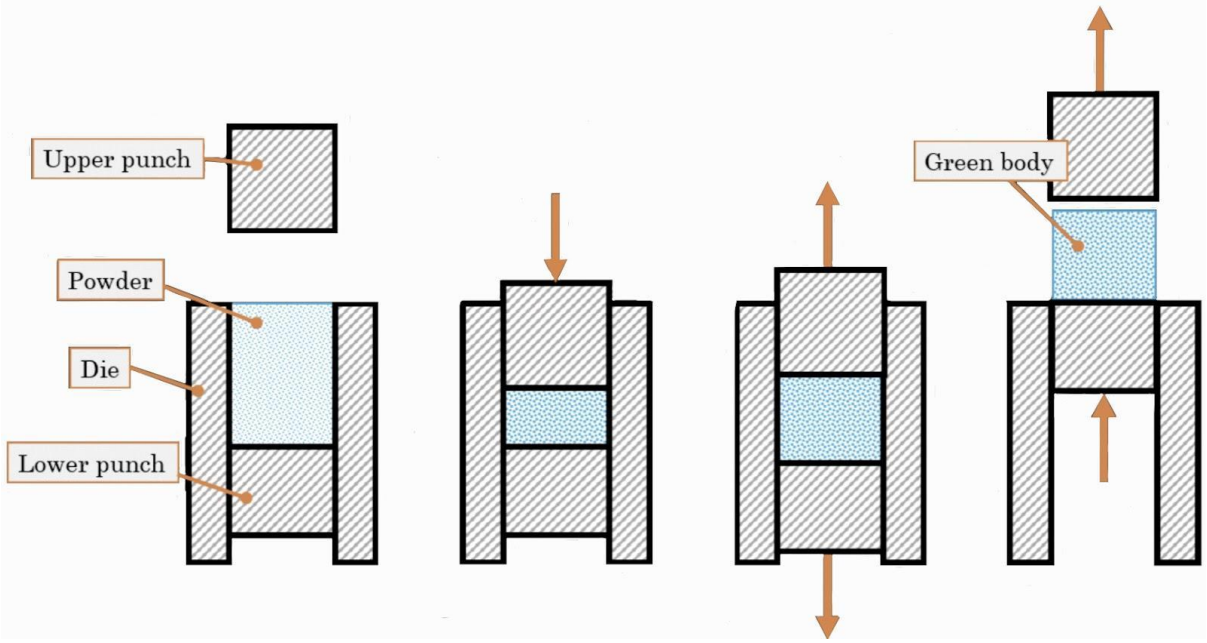

Figure 1, Schematic figure of the pressing process of the green body

2.4 Flowability

The flowability of a powder defines the powder's flow properties related to the powder particles' cohesion.[10]. The powder's flowability is affected by many factors, such as the particle's shape, size and distribution. Environmental factors like humidity, temperature, and particle interaction forces like

friction also affect flowability [11]. A particle's flow properties are enhanced by a smooth surface, whereas a rough surface results in poor flowability due to increased friction [12]. High interparticle forces refer to a poor flow and vice versa. The flowability of a powder will affect its compressibility as it determines the ability of the powder to fill the cavities of the punches and die [9].

2.5 Compressibility and Compactibility

Measuring the densification of a powder under an applied pressure is called compressibility. The powder is filled in a die with a set density, then compressed and shaped. After the powder is compacted, the so-called green density is measured, which is the basis for expressing the compressibility. Compactibility is linked to the rearrangement of particles when forming the green body during pressing [9]. In this thesis, "compaction properties" is defined as the rearrangement of powder during compaction, measured by looking at the shape distortion on a sintered part.

2.6 Powder Characterisation

2.6.1 Hall Flow and Apparent Density

The Hall flow meter used is a device produced by Qualtech (Products Industry Ltd, Denver, Co, USA). It is developed to measure the flowability and density of a powder. The powder flowability is measured by timing how long it takes for the powder to go through the Hall flow funnel. The funnel had a 30 degree conic half angel, 25.4 mm diameter hole and some roughness following the standard A powder's speed indicates the friction between the particles in the powders. It was decided with the industrial partners that 25 ml of powder was to be used for the test, instead of the standard 50 g as the powders have a high density. This density of the powder can be found by weighing it, as the volume is known [9].

2.6.2 Particle Size Distribution

Particle size distribution (PSD) gives information about the size and shape of particles. There are different ways of determining these data, some old styles, like sieving, and some more recent, like image analysis. The latter will be used in this project.

The machine used is QICPIC (SympaTec GmbH, Clausthal-Zellerfeld, Germany) using compressed air dispersion by a RODOS dispersion module. The powder is placed in a funnel of the QICPIC, and the funnel controls the feed of powder to the disperser, which vibrates to spread the powder out. The powder then arrives in front of the air compressor, which shoots it in front of the camera. The camera takes a picture of the particle's shadow, which gives data on the particle's shape and size. It is the most recent way of measuring the PSD, being available for less than 20 years, but significant because it is fast, accurate and gives much information on the size previously unavailable. The measured range can theoretically go from 1.8 µm to 3.755 mm (from 1 pixel to the diameter of the tube). However, the ISO standard (ISO 13322-1/2) accepts less to assess the accuracy (from 16 µm to 1,3 mm), and the shape can be accurately described only from 5µm as it needs 9 pixels and not one [13]. A common problem is if the particles are not spherical, as it will be difficult to characterize the size by one number. Also as this method relies on pictures, every descriptor comes from a 2D image of the

particle. Another problem is to have a representative sample, as it is easy to shift the curve by missing the biggest or smallest particles [9].

2.6.3 The Angle Of Repose

The angle of repose refers to the maximum angle at which the material of a granular solid can be piled on a flat surface without collapsing. In general, the angle of repose is used in many different applications such as design processing and storage, for instance, storage bins in the food industry [14].

The value of the angle of repose depends on several factors, such as the particle's size, shape, and smoothness. Materials with smooth and spherical granules result in a low angle and are highly flowable. In contrast, sticky and fine materials have a high angle of repose [15].

2.6.4 Tapped Density

Tapped density is a variant of density defined as the ratio of the mass by tapped volume. This volume is achieved after tapping a powder a certain number of times [16]. The method involves placing the powder in a graduated cylinder. The graduated cylinder is connected with an instrument mechanically tapping the powder between 284 and 3000 cycles per minute. When the desired number of taps is reached, the machine is stopped, and the new volume is measured [9].

The density of the powder will increase fast at the beginning before plateauing. Tap density is an important physical property in many industries, such as metal powder manufacturing and pharmaceutical research, where it is essential to understand powder flowability and compaction properties [16]. The phenomenon is the maximum density achieved by tapping a metal powder under certain conditions [17]. More regularly shaped particles result in a high value of the tap density compared to irregularly shaped particles resulting in a low value of the tap density [16].

2.6.5 Powder Rheometry

The FT4 Powder Rheometer (Freeman Technology Ltd, Tewkesbury, UK) is a universal powder tester used to characterize powder flow properties and powder behavior. It can make a lot of different tests; the ones that will interest us are mainly the shear test and the stability and variable flow rate test [18]. The latter uses a blade that rotates at an angle in the powder. As the blade goes down, it compresses the powder and maximizes the friction between particles. The rheometer measures the energy needed to maintain the speed of the blade. It can be argued that more energy means more cohesive forces, as the blade traverses the same distance with the same speed for each powder.

During the shear test, a shear force at a slow speed is applied to the powder. A large force is applied and it decreases until the motion stops, measuring the shear strength of the powder. The cohesion is then measured by taking the intersection between the y-axis and the slope of the measurements and show the shear stress with no normal stress applied. The Free Flowing index is calculated by constructing two Mohr circles from the results of the test and finding the ratio between their intersection with axis x, $FF = \frac{b}{a}$. A higher index indicates a higher flowability, the flow is denoted good if higher than 10 [19].

2.7 Powder Composition

Sandvik Coromant provided the powder composition. The powder was then renamed depending on its different types and percentage of PEG.

Table 1, Composition of the Powders

Powder name	PEG amount (wt%)	PEG hardness	Note:
H 2.0 I	2	hard	Mixture of 3 PEG
H 2.0 II	2	hard	Mixture of 3 PEG
H 2.0 III	2	hard	Mixture of 3 PEG
S 2.0	2	soft	Mixture of 3 PEG
S 1.0	1	soft	Mixture of 3 PEG
H 1.0	1	hard	Mixture of 3 PEG
VH 1.0	1	very hard	Mixture of 3 PEG
H 2.0 2P	2	hard	Only Two types of PEG
M 1.5 EA	1,5	medium	Erucic Acid 0.5wt% + Mixture of 3 PEG
M 1.5 OA	1,5	medium	Oleic acid 0.5wt% + Mixture of 3 PEG
M 1.5 Sp	1,5	medium	Spherical cobalt + Mixture of 3 PEG
M 1.5	1,5	medium	Mixture of 3 PEG

3. Method

3.1 Powder Characterisation

3.1.1 Hall Flow and Apparent Density

Each powder was poured into a cup with a volume of 25 ml. The cup was leveled using a ruler to get an exact amount. The cup and the powder were then weighed, using a Presica 321 LX 2200C scale, to calculate the density of the powder which was done by dividing the volume of the cup, 25 ml, by the weight of the powder. Further, the powder was poured into the Hall Flow funnel. A finger was placed under the funnel at the outlet hole while the metal powder was poured into the funnel. A stopwatch was started at the same time as the finger was released from the funnel. The timer was stopped when all the powder had passed through the funnel, and the time was noted. The funnel was cleaned with a brush between each of the powder tests. The measurements described above were performed three times for each powder to obtain the most accurate results possible. The tests were carried out in a fume cupboard to avoid spreading the powder around the lab due to its cobalt content.

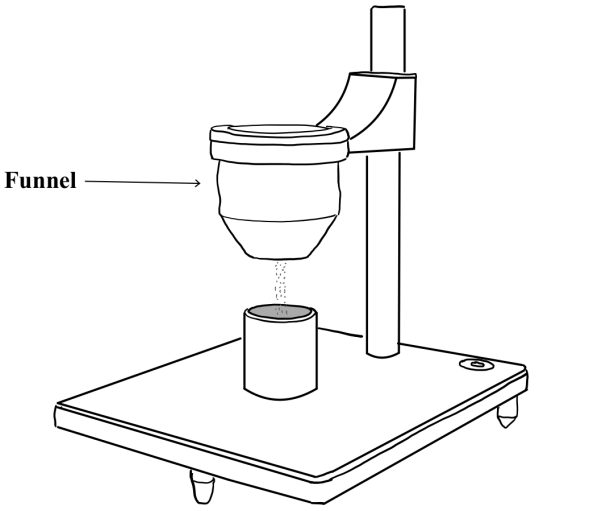

Figure 2, Hall flowmeter

3.1.2 Particle Size Distribution

The machines used for this test are the SympaTec QICPIC [13]. Compressed air was used to spray the particles in front of the camera. The airflow pressure was set to 0.5 bar, to avoid breaking the particles. A metal spoon was used to pour each powder into a funnel of the machine. It led down to a gutter where the metal powder was transported by vibration to disperse the particles. The powder then arrives on a compressor which uses airflow to propel the particles in front of a laser beam that illuminates all the particles and the camera takes pictures of these. The computer receives and analyzes the images to find relevant measurements and metrics.

Diameter: Diameter of a circle of equal projection area (EQPC). The area of the particle is measured and the diameter of a circle with the same area is computed. It is useful as we want to be able to compare particles with various shapes.

Aspect ratio: The aspect ratio is the particle's smallest diameter ratio compared to its larger diameter. (= 1 if circle)
Convexity: Convexity is the relative amount that a particle differs from a convex shape. It is computed by the ratio between the area of the particle and the area of its closest convex shape (= 1 if convex, less if not).
Sphericity: Sphericity is the degree to which an object approaches an ideal "sphere". It is computed by the ratio between the perimeter EQPC (from the earlier computed diameter) and the actual perimeter of the particle (= one if spherical particle, less if not) [20]. These last three metrics indicate useful information to approach the shape of the particle.

3.1.3 Angle Of Repose

The powders were weighed to 100 grams and then poured into the angle of repose measurement equipment (Qualtech Products Industry, Denver, Co, USA). Using a finger, the powder was stopped from going out of the outlet hole in the bottom of the funnel until all the powder was poured into it. When the powder flowed through, it created a cone on a round plate under the cup. Using a protractor built into the instrument, the angle of the cone could be measured at three different points, situated at 120° from each other around the base of the pile. In order to get these measurements, the plate on which the powder lay was turned. Each of the powder was tested three times with a new powder for each test.

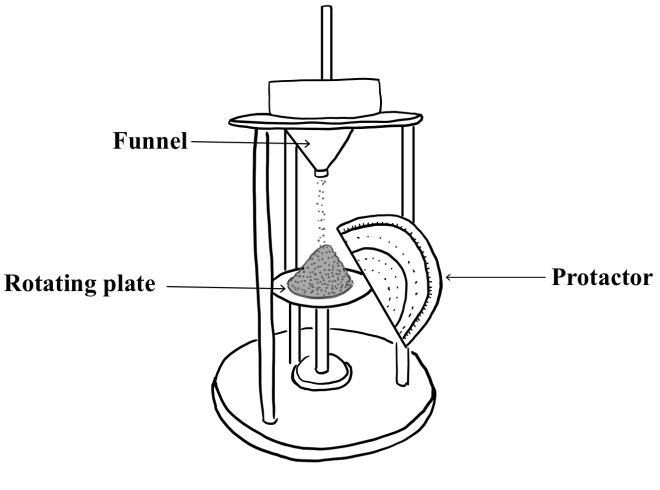

Figure 3, Angle Of Repose

3.1.4 Tapped Density

Tapped density tests were performed in accordance with ISO 3953:2011 using a dedicated machine (Quantachrome Autotap. Anton Paar Nordic AB, Malmö, Sweden). 50 g of powder was placed into a measuring cylinder to measure the volume of the powder. The top of the cylinder was then sealed to prevent powder from flying out, and the cylinder was attached to the tapping machine. The mechanical tapping was stopped, and the volume of the powder was measured after 5, 10, 25, 40, 75, 200, 1000, and 3000 taps, as requested by the industrial partner. Each powder was tested twice with new powder used for each test.

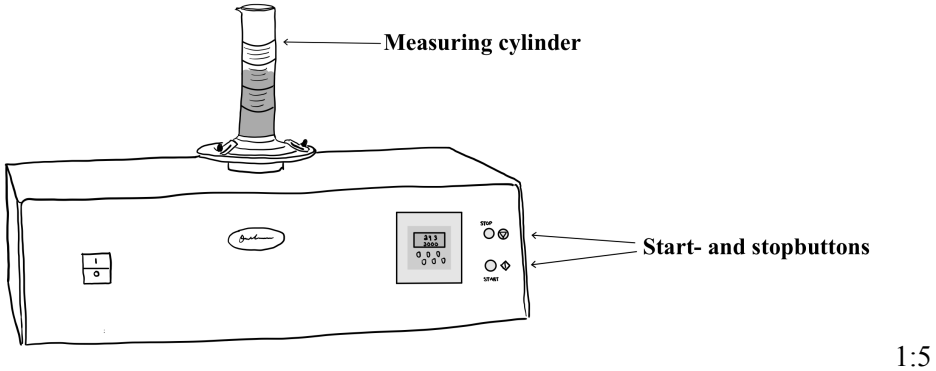

Figure 4, Tap Density

3.1.5 Powder Rheometry

The first test using the Freeman FT4 Powder Rheometer (Freeman Technology, Ltd., Tewkesbury, UK) was the stability and variable flow rate. This test uses a two-piece glass tube of 25 mg each. The tube was pre-weighed and then filled with the respective powder. After the machine weighed the glass container with the powder, the process started with a thin metal shaft equipped with a blade stirring the powder. Once the powder was thoroughly stirred, the two parts of the glass tube were separated, and the excess powder that sat in the upper part of the cylinder was removed to level the lower cylinder. Then eleven test sequences were performed on the powder to measure its resistance against the blade. The first seven tests were under identical conditions and are designed to test if the powder changes behavior under repeated testing. The final four tests use different speeds of the metal blade that is driven though the powder to test if the powder responds differently to the different speeds.

The Rheometer was also used to do a shear cell test. This test uses a different two-piece glass tube the lower of which is a known volume of 10 ml. The powder was stirred with the metal blade, which was then replaced by a plastic press to compress the powder. When the powder was finished being pressed, the glass tube was opened to level the powder in the 10 ml tube. The plastic press was changed to a metal press with built-in “vanes” to dig into the powder. The test head was rotated under a defined axial load to find the shear force at which the powder stopped flowing. This was repeated under different axial loads to build up a dataset of shear stress as a function of compressive stress.

3.2 Measurements of the inserts

A micrometer was used to measure the inserts (Teng Tools AB, Alinsås, Sweden). The goal of the measurement was to determine the lowest and highest points of the insert to get a measurement of the powder's compressibility. The lowest point of the insert was measured at its center. The highest point was obtained by calculating an average from the heights of the three different peaks of the inset. To ensure that the measurements were as accurate as possible, they were taken by all members of the group. The different measurement values for each insert were then calculated to an average. To obtain each insert’s ratio between its lowest and highest points, the lowest value was divided by the average of the highest.

3.3 Calculation of Errors

All measurements come with an error due to the maximum precision of the instrument or the human factor. The natural variation in a given population is also encountered by doing averages. These errors need to be taken into consideration when analyzing results. For that, some statistical calculations must be done when adding, multiplying, or dividing results. This is called the propagation of errors [21].

For addition: $a + b - c = x \rightarrow$

$$\sigma_x = \sqrt{\sigma_a^{\,2} + \sigma_b^{\,2} + \sigma_c^{\,2}} \qquad \text{Eq. 1}$$

For multiplication/division: $\frac{ab}{c} = x$

$$\frac{\sigma_x}{x} = \sqrt{\left(\frac{\sigma_a}{a}\right)^2 + \left(\frac{\sigma_b}{b}\right)^2 + \left(\frac{\sigma_c}{c}\right)^2} \qquad \text{Eq. 2}$$

In the equations above, a, b, and c are the measured variables and σ_a, σ_b, and σ_c are the errors of those variables.

4. Results

4.1 Powder Characterisation

4.1.1 Hall Flow and Apparent Density

Table 2 shows results for an average of weight, density, time and time per weight for the three rounds of testing for each metal powder. In Figure 5 the time in Table 2 is plotted, including the error where the biggest one is the standard deviation between the three tests on average 0.5 seconds. Figure 6 represents the time for 1 gram to go through the funnel, in this case the biggest error is calculated using Eq. 2 on the instrumental error of the scale and the human reaction time for the stopwatch.

Table 2, Hall Flow

Sample	Weight (g)	Density (g/ml)	Time (s)	Time per weight (s/g)
H 2.0 I	88,18	3,53	40,33	0,4574
H 2.0 II	86,88	3,48	42,19	0,4856
H 2.0 III	84,39	3,38	39,08	0,4631
S 2.0	83,91	3,36	40,35	0,4809
S 1.0	81,84	3,27	45,38	0,5545
H 1.0	83,62	3,34	42,79	0,5117
VH 1.0	84,64	3,39	41,00	0,4844
H 2.0 2P	87,68	3,51	38,77	0,4422
M 1.5 EA	95,53	3,82	41,96	0,4392
M 1.5 OA	95,41	3,82	39,67	0,4158
M 1.5 Sp	84,99	3,40	41,46	0,4878
M 1.5	84,18	3,37	40,83	0,4850

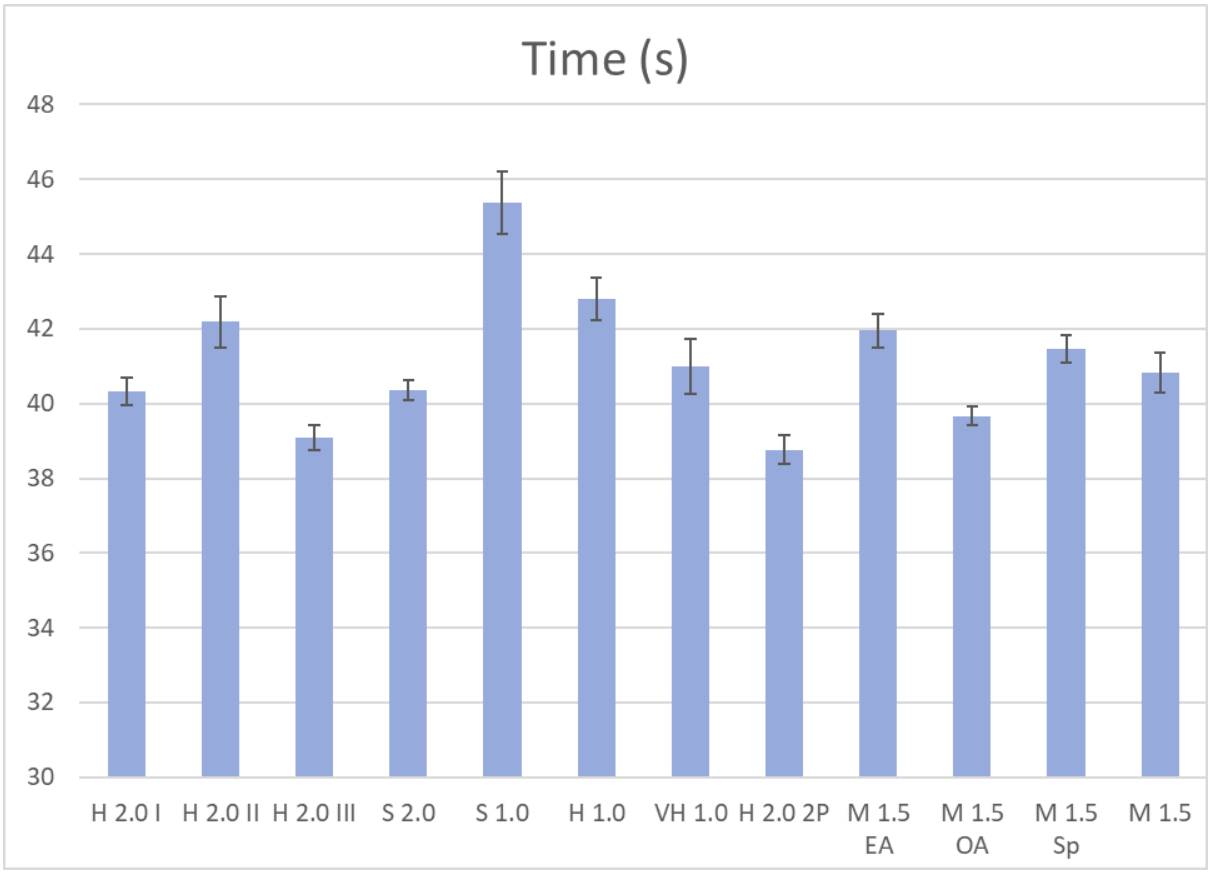

Figure 5, Hall flowtime and error calculation

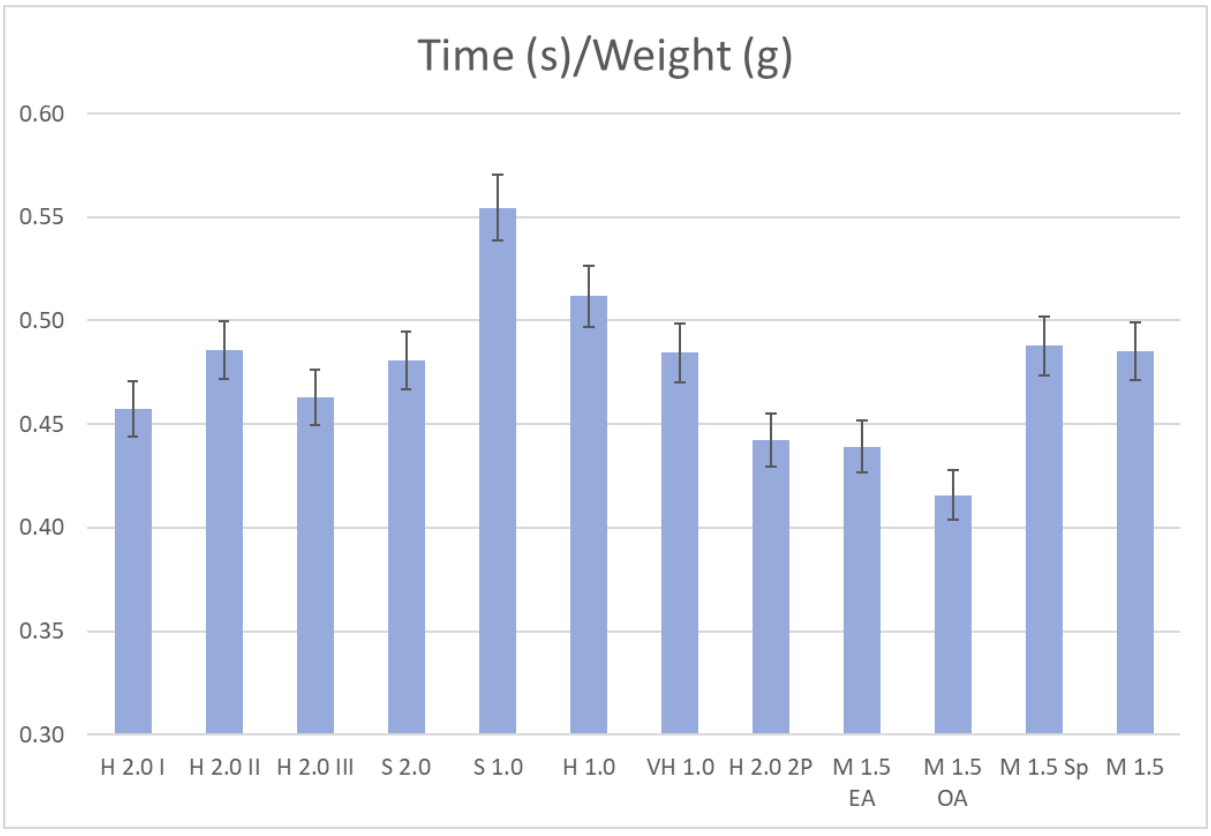

Figure 6, Hall flowtime divided by weight and error calculations

4.1.2 Particle Size Distribution

The letter d in Table 3 is the diameter EQPC. The number after the d is the proportion of particles below this size, thus d50 is the median. The span of the distribution,*n,* can be calculated using Eq. 3 to show the size's spread. If the spread is small, *n* will also be small, thus creating a sharp peak. Figures 8 and 9 are graphs given by the software. One curve, with up and downs, represents the proportion of particles present for each size. The second curve is always rising as it represents the cumulative distribution, d10, 50 and 90 come from this curve. A spoon of powder was used for each test, which while not a precise measure gives results for roughly a million particles, which is enough to give data with a high level of confidence.

$$n = \frac{(D90 - D10)}{D50} \qquad \text{Eq. 3}$$

Table 3, Particle Size Distribution

Powder	d10 (µm)	d50 (µm)	d90 (µm)	n	Observation
H 2.0 I	52,91	99,67	171,8	1,19	1 wide peak
H 2.0 II	55,9	108,75	183,03	1,17	1 wide peak
H 2.0 III	16,49	79,4	136,69	1,51	1 big peak
S 2.0	8,24	52,69	123,88	2,19	small 1st, big 2nd
S 1.0	6,05	17,11	109,65	6,05	1st big peak, then plateau and slight 2nd peak
H 1.0	6,94	40,63	125,29	2,91	2 peak, 2nd slightly bigger
VH 1.0	7,52	51	130,76	2,42	small 1st, big 2nd
H 2.0 2P	24,13	81,6	132,81	1,33	1 big peak
M 1.5 EA	8,36	54,55	112,93	1,92	small 1st, big 2nd
M 1.5 OA	8,03	55,46	119,11	2	small 1st, big 2nd
M 1.5 Sp	7,57	48,89	133,42	2,57	small 1st, big 2nd
M 1.5	7,18	40,25	120,05	2,8	2 peak, 2nd slightly bigger

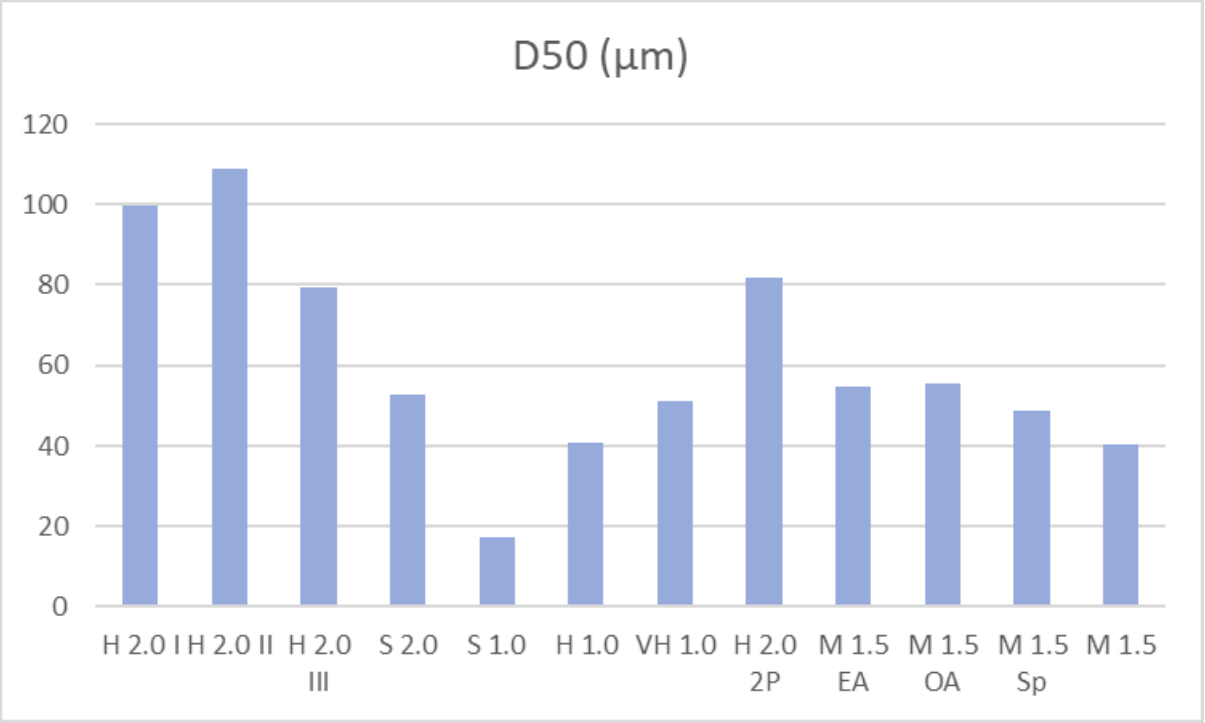

Figure 7, Median diameter of particles

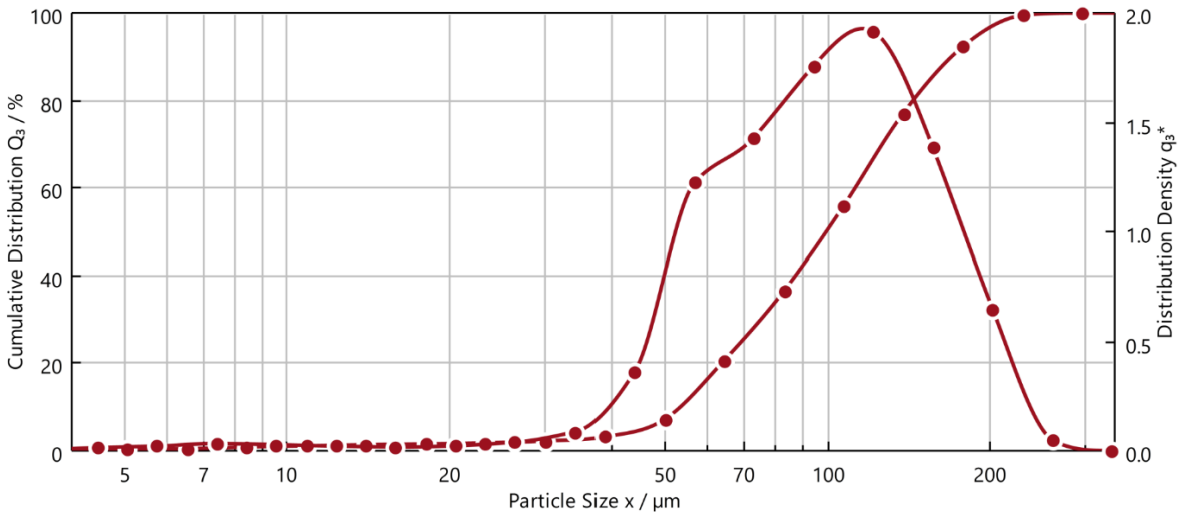

Figure 8, PSD graph of H 2.0 I

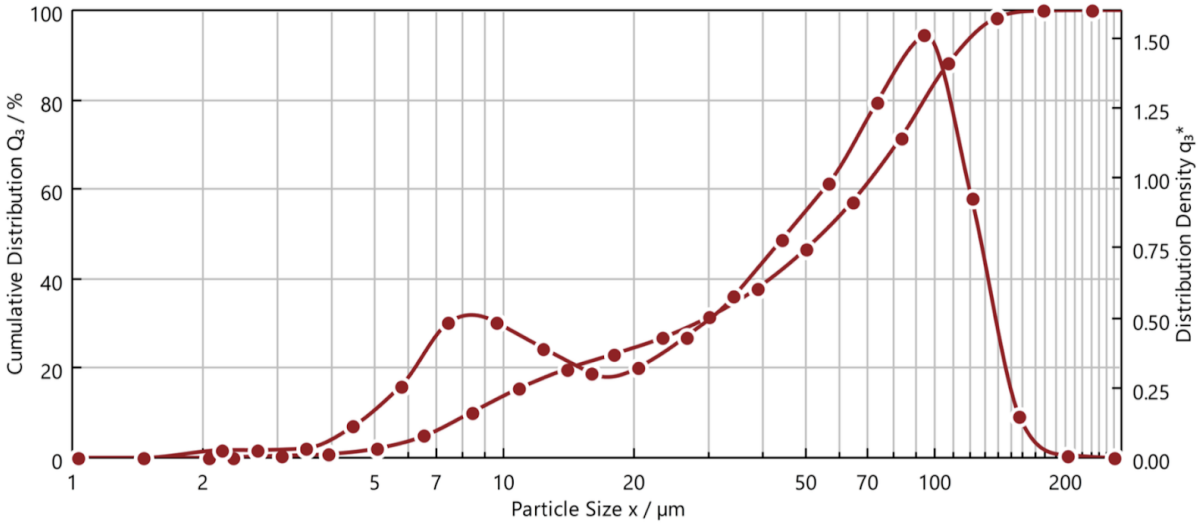

Figure 9, PSD graph of M 1.5 EA

All the values in Table 4 come directly from the image analysis. Figure 10 shows the variation of the mean aspect ratio depending on the powder, while Figure 11 shows the variation in one powder depending on the size of the particles.

Table 4, Values from the image analysis

Powder	Mean aspect ratio	Median aspect ratio	Deviation aspect ratio	Mean sphericity	Median sphericity	Deviation sphericity	Mean convexity	Median convexity	Deviation convexity
H 2.0 I	0,89	0,92	0,09	0,85	0,85	0,07	0,94	0,95	0,03
H 2.0 II	0,95	0,95	0,03	0,85	0,85	0,06	0,95	0,95	0,03
H 2.0 III	0,84	0,88	0,11	0,85	0,85	0,07	0,93	0,94	0,04
S 2.0	0,8	0,82	0,12	0,85	0,85	0,07	0,91	0,92	0,05
S 1.0	0,75	0,75	0,12	0,85	0,87	0,1	0,89	0,9	0,07
H 1.0	0,78	0,79	0,12	0,84	0,85	0,09	0,9	0,91	0,06
VH 1.0	0,79	0,81	0,12	0,84	0,85	0,08	0,91	0,92	0,05
H 2.0 2P	0,85	0,89	0,11	0,85	0,85	0,07	0,93	0,94	0,04
M 1.5 EA	0,8	0,82	0,12	0,85	0,85	0,08	0,91	0,92	0,05
M 1.5 OA	0,8	0,82	0,12	0,85	0,85	0,08	0,91	0,92	0,05
M 1.5 Sp	0,79	0,81	0,12	0,85	0,85	0,08	0,91	0,92	0,05
M 1.5	0,78	0,8	0,12	0,85	0,86	0,08	0,91	0,91	0,05

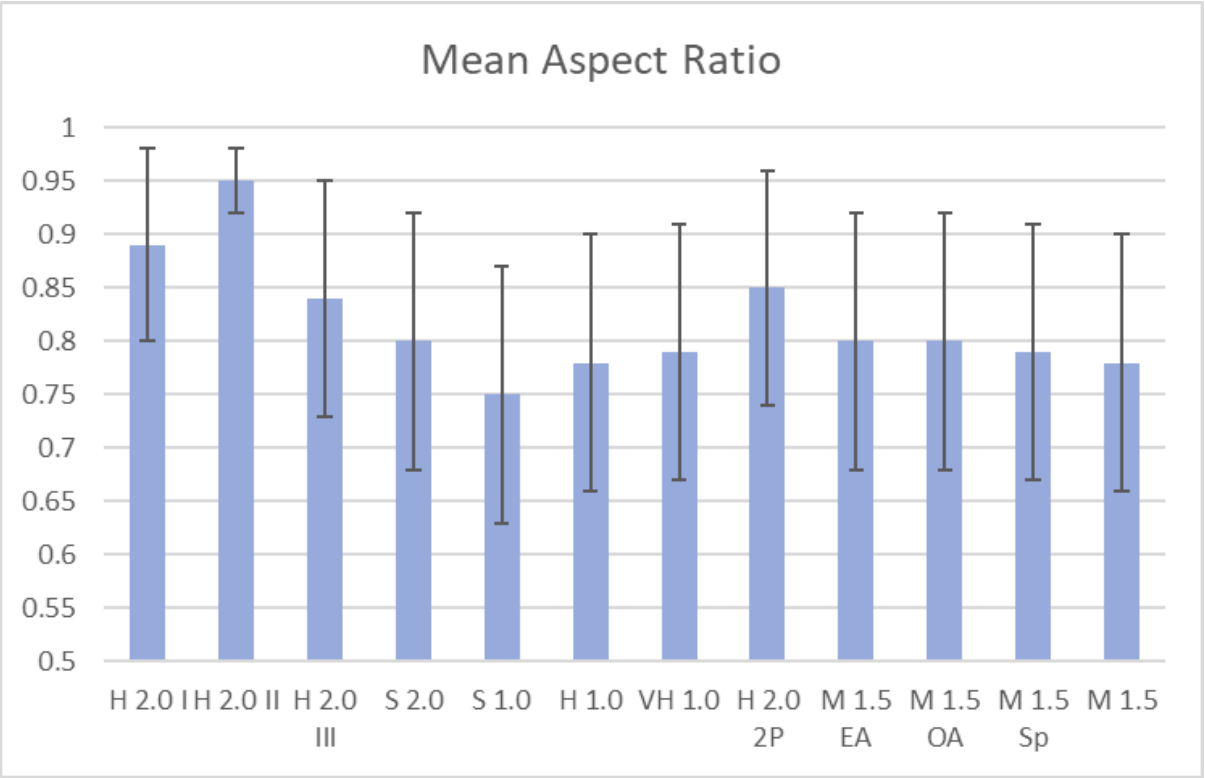

Figure 10, Mean Aspect Ratio of powders with deviation

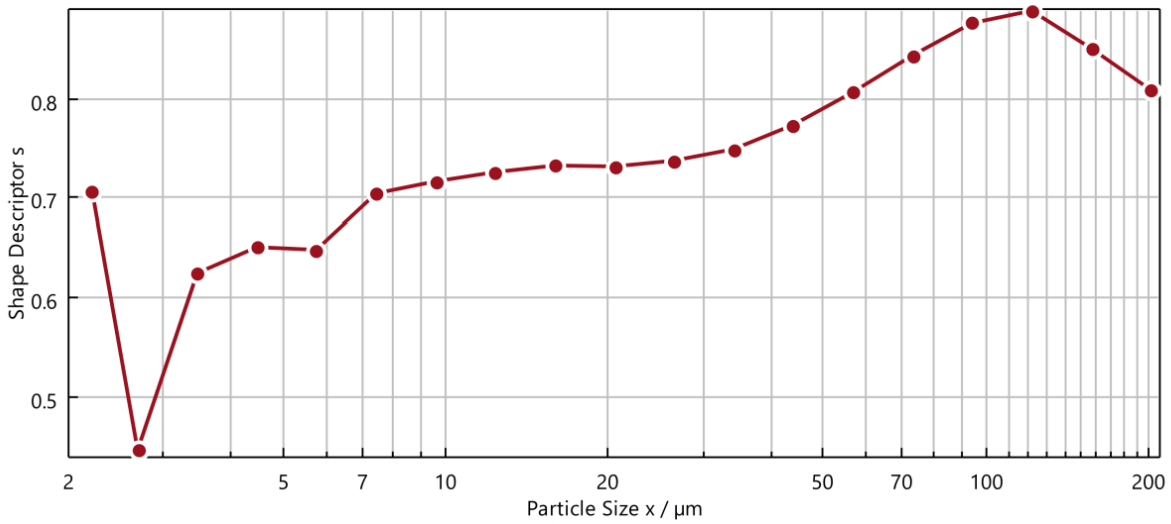

Figure 11, Aspect ratio on particle size for powder M 1.5 EA

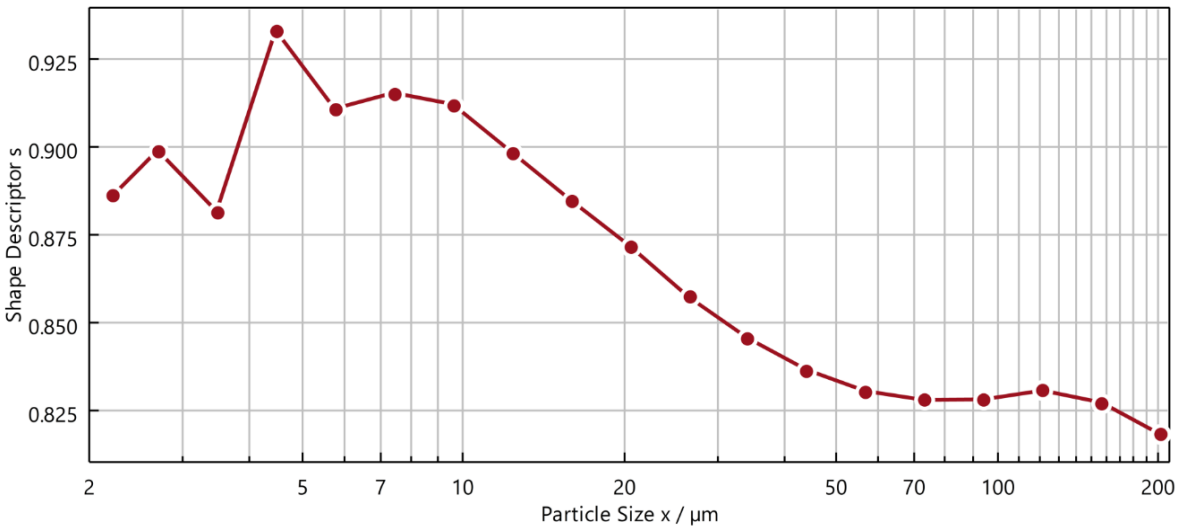

Figure 12, Sphericity on particle size for powder M 1.5 EA

4.1.3 The Angle Of Repose

The test was repeated three times with each powder and three angles were measured each time, Table 5 and Figure 13 show the average and standard deviation of the nine angles, the error of the instrument, of the order of 1 degree, is negligible compared to the scattering of the result which is present as the standard deviation.

Table 5, Average and standard deviation of the angles

Powder	**Average angle**	**Standard deviation**
H 2.0 I	30	1,155
H 2.0 II	26,67	1,944
H 2.0 III	25	1,633
S 2.0	27,78	1,397
S 1.0	33	1,886
H 1.0	30,44	1,423
VH 1.0	27,67	1,054
H 2.0 2P	26,39	1,487
M 1.5 EA	28,44	2,061
M 1.5 OA	25,33	2,055
M 1.5 Sp	28,39	2,836
M 1.5	29,33	0,816

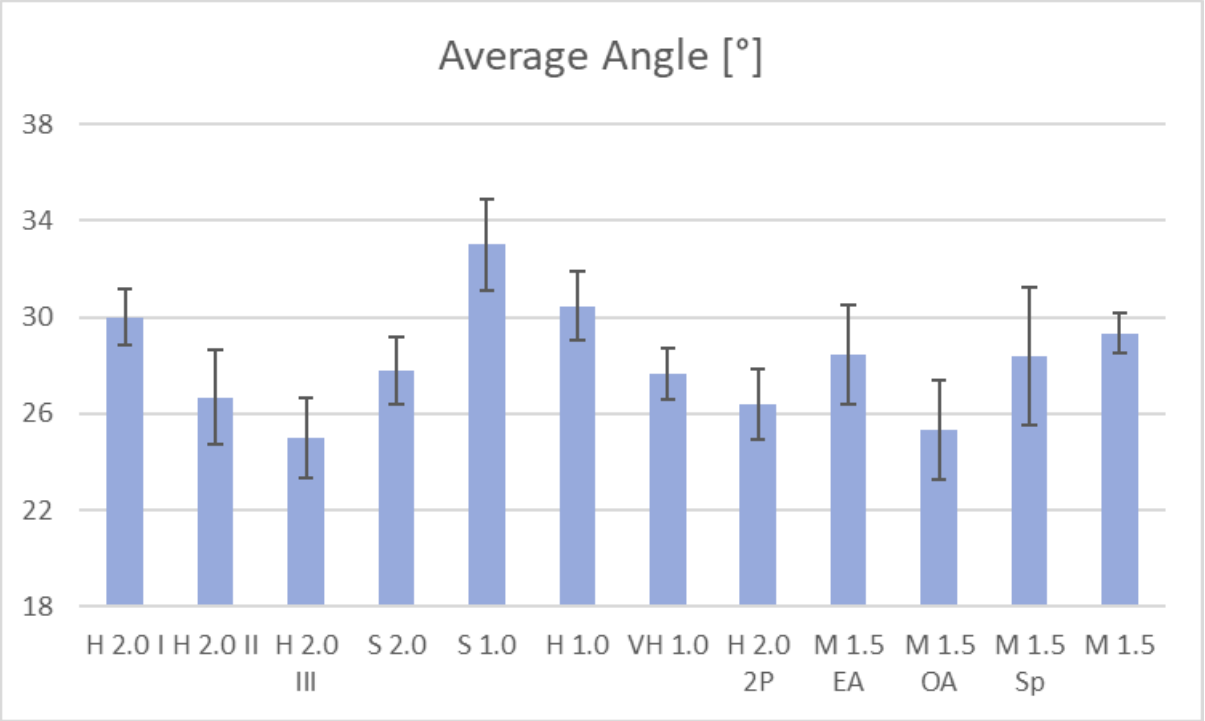

Figure 13, Average angle of the powders

4.1.4 Tap Density

The tap density test was done two times for each powder. Fifty grams of powder were used each time, and its volume before and after tapping was noted. The weight divided by the volume gives the density. Then the average of the two measurements was noted in Table 6 and plotted in Figure 14. The error was computed by the propagation of errors from the scale's precision (+/- 0.05 g) and volume measurement (+/- 0.1 ml) or by the standard variation between the two tests, depending on the highest. Table 6 and Figure 15 also show the Hausner ratio, it is the ratio of the tap density to the apparent density. The error is given by the propagation of errors from the instrumental precision.

Table 6, Measurements of the Tap Density and Hausner ratio

Powder	Density 0 tapp	Error	Density 3000 tapps	Error	Hausner ratio	Standard deviation
H 2.0 I	3,472	0,0241	3,984	0,0197	1,1474	0,008
H 2.0 II	3,46	0,0171	3,906	0,0193	1,1289	0,0079
H 2.0 III	3,367	0,0162	3,718	0,0415	1,1042	0,0075
S 2.0	3,356	0,0451	3,803	0,0434	1,1331	0,0077
S 1.0	3,215	0,0148	3,939	0,0931	1,2250	0,008
H 1.0	3,3	0,0156	3,937	0,031	1,1930	0,008
VH 1.0	3,333	0,0159	3,847	0,0592	1,1541	0,0078
H 2.0 2P	3,413	0,0349	3,984	0,0194	1,1674	0,008
M 1.5 EA	3,718	0,0197	4,425	0,0234	1,1903	0,0089
M 1.5 OA	3,69	0,0194	4,386	0,023	1,1886	0,0088
M 1.5 Sp	3,322	0,0158	3,922	0,0186	1,1804	0,0079
M 1.5	3,333	0,0222	3,953	0,0188	1,1858	0,008

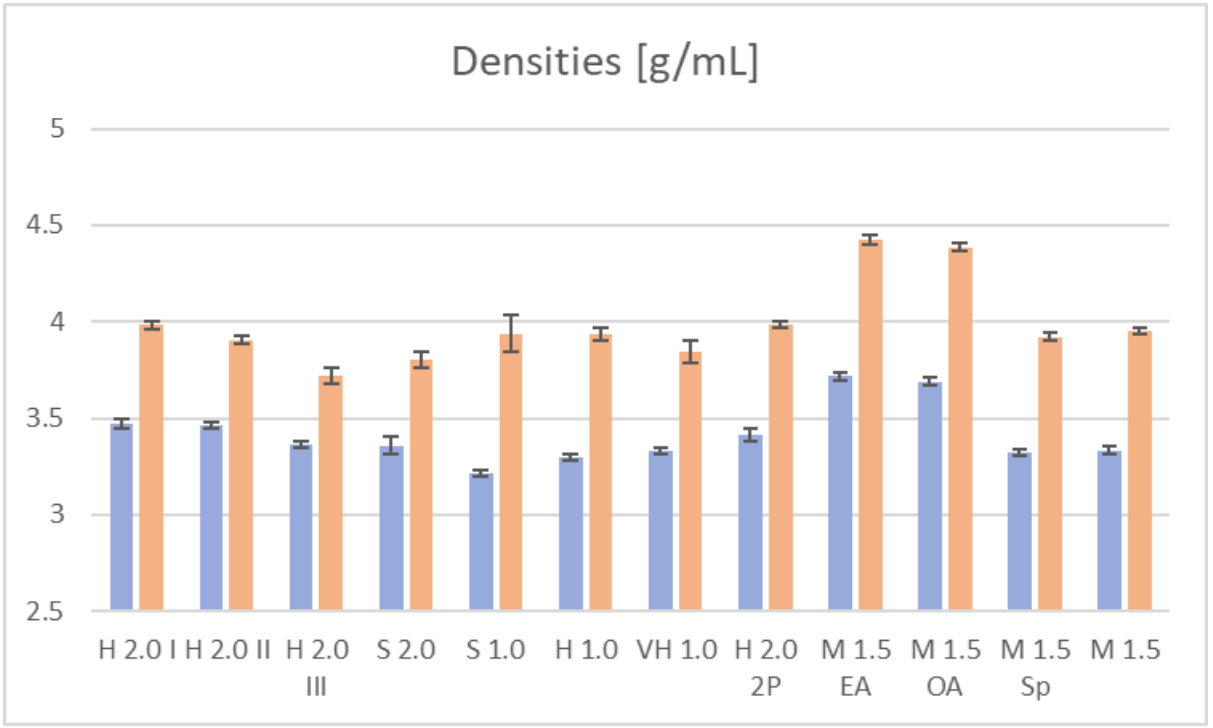

Figure 14 Apparent (blue) and tap (orange) densities

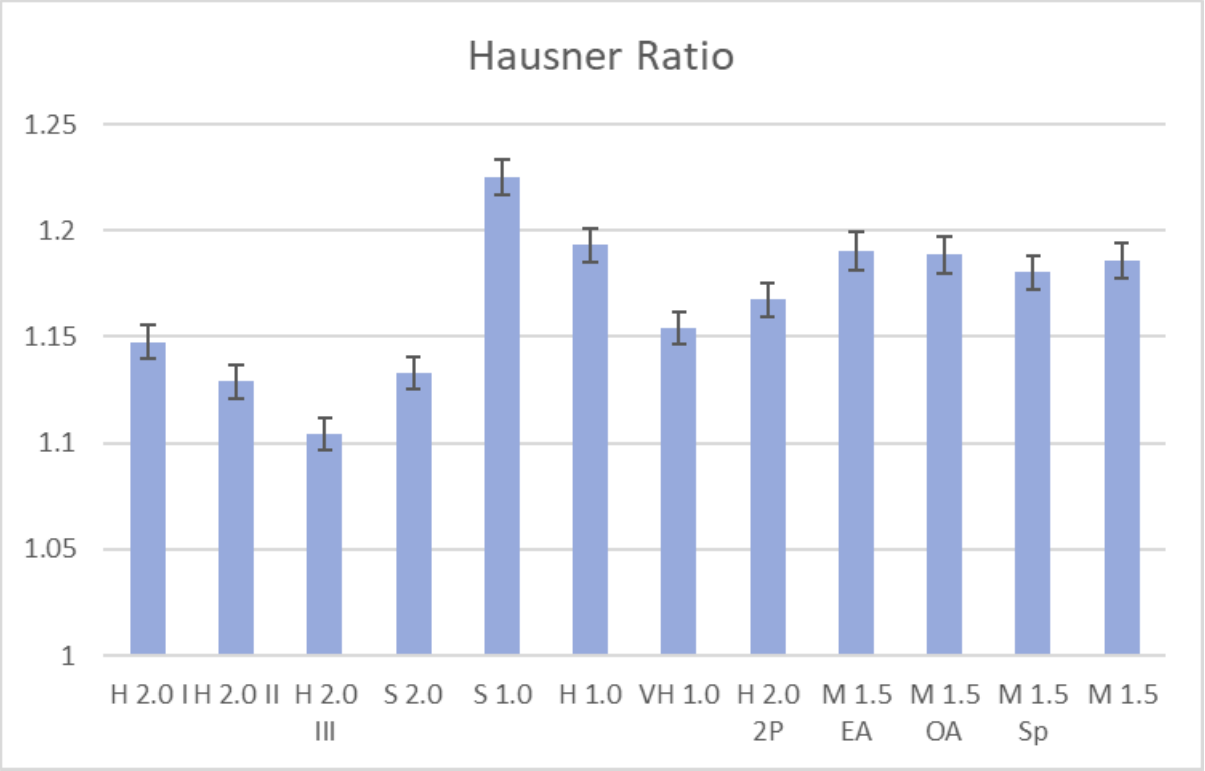

Figure 15, Hausner ratio

4.1.5 Rheometer FT4

Figure 16 shows the behavior of the respective twelve metal powders during a test with a rheometer. The x-axis indicates that the powders were subjected to one test with 11 different test runs at varying speeds of the spinning blade. The y-axis shows the energy generated by the test.

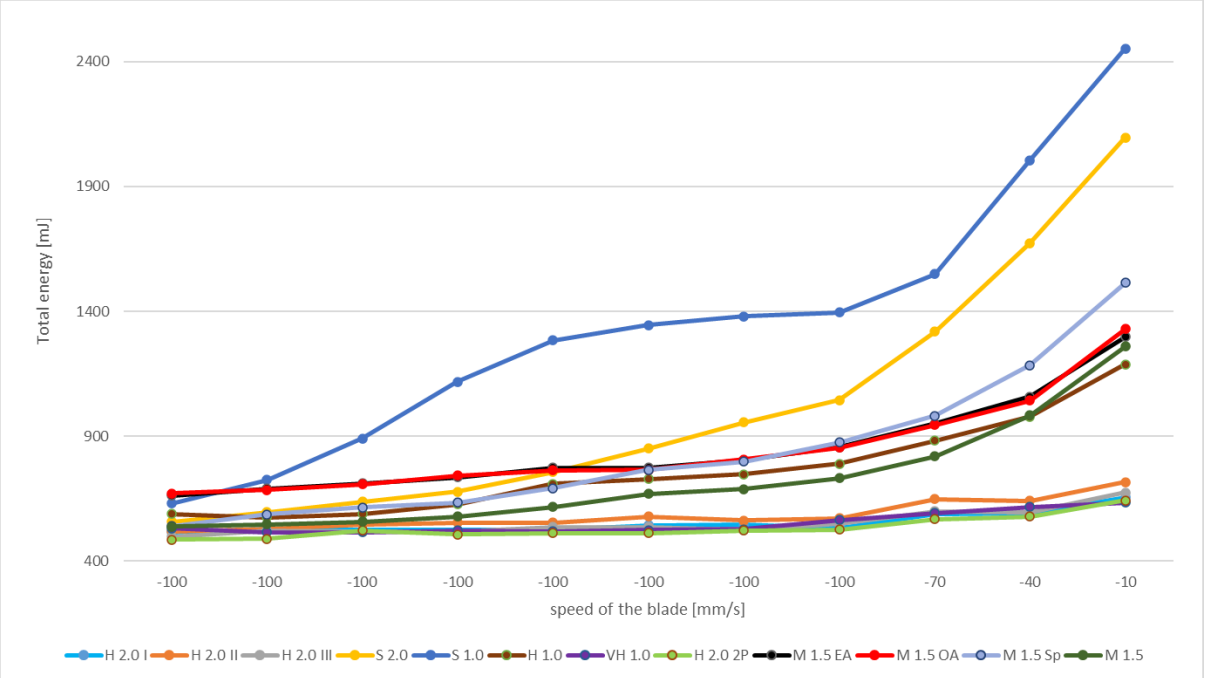

Figure 16, Measurements of the flowability, total energy (mJ) on the speed of the blade (mm/s)

Figure 17 shows the behavior of the respective twelve metal powders during a test with a rheometer, performing a shear test. The x-axis indicates that the powders were subjected to 6 test rounds at varying shear normal stress. The y-axis shows the shear stress generated by the stress.

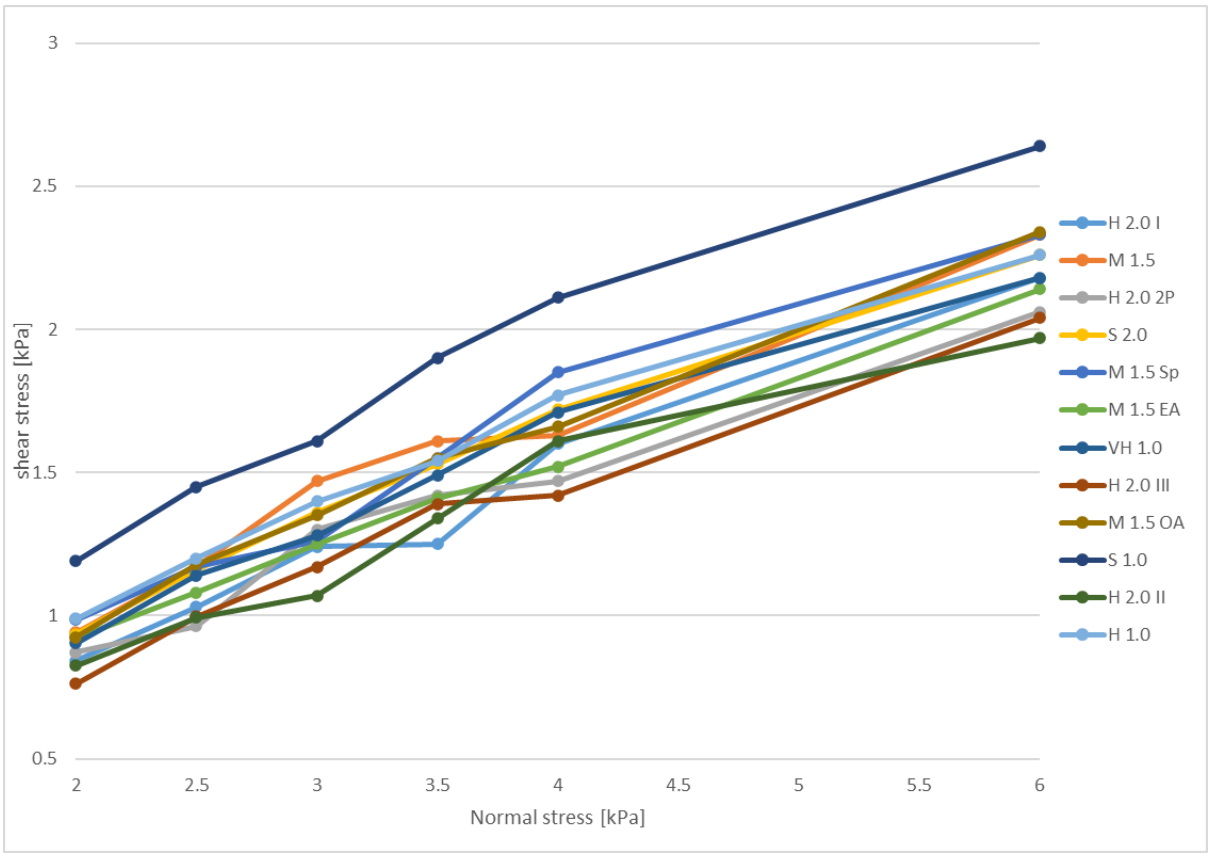

Figure 17, Measurements of the shear stress (kPa) on normal stress applied (kPa)

Figure 18 shows the variation of the Free Flowing index. The cohesion in Figure 19 is the shear stress when no force is applied [22].

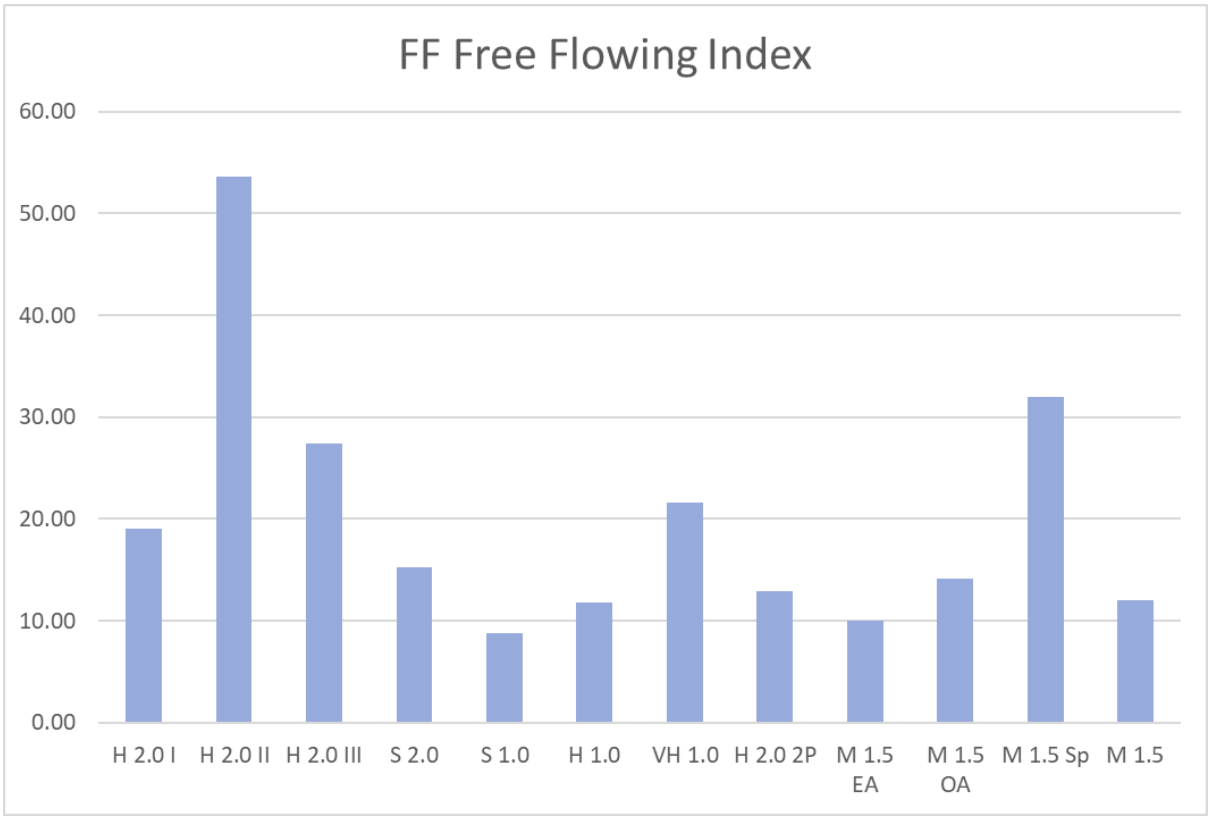

Figure 18, Free Flowing index

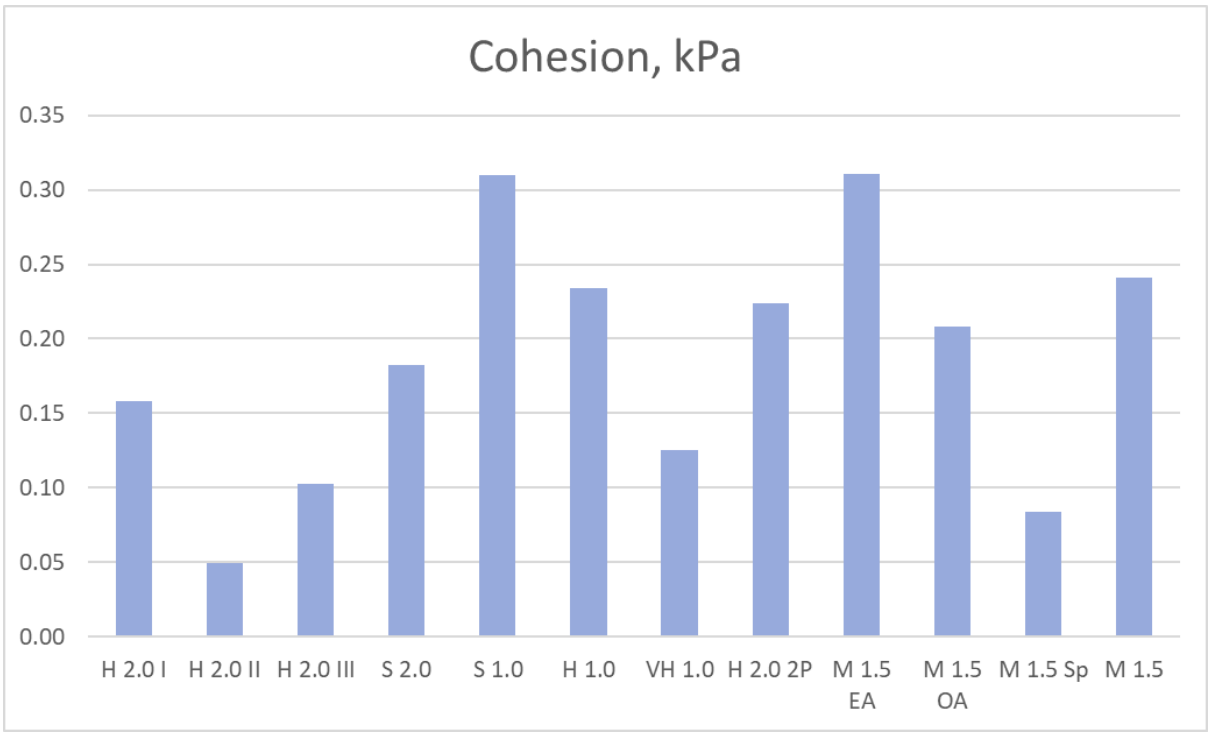

Figure 19, Cohesion of each powder

4.2 Measurements of the inserts

Table 7 and Figure 20 show the measurements of the inserts produced by the different powders. The a value represents the lowest point of the insert, and the b value is its highest point. To calculate which insert had the most significant ratio between a and b, equation 4 was used. The error comes from the standard deviation of the ratio calculated by the different measurements on the samples.

$$Ratio = b/a \quad \text{Eq. 4}$$

Table 7, The measurements of the inserts

Powder	**a**	**b**	**Ratio**
H 2.0 I	4,93	7,11	1,4430
H 2.0 II	4,93	7,11	1,4428
H 2.0 III	4,92	7,1	1,4431
S 2.0	4,9	7,1	1,4490
S 1.0	4,89	7,08	1,4473
H 1.0	4,93	7,12	1,4448
VH 1.0	4,43	7,11	1,4437
H 2.0 2P	4,92	7,1	1,4422
M 1.5 EA	4,93	7,15	1,4498
M 1.5 OA	4,94	7,15	1,4473
M 1.5 Sp	4,93	7,12	1,4459
M 1.5	4,92	7,11	1,4462

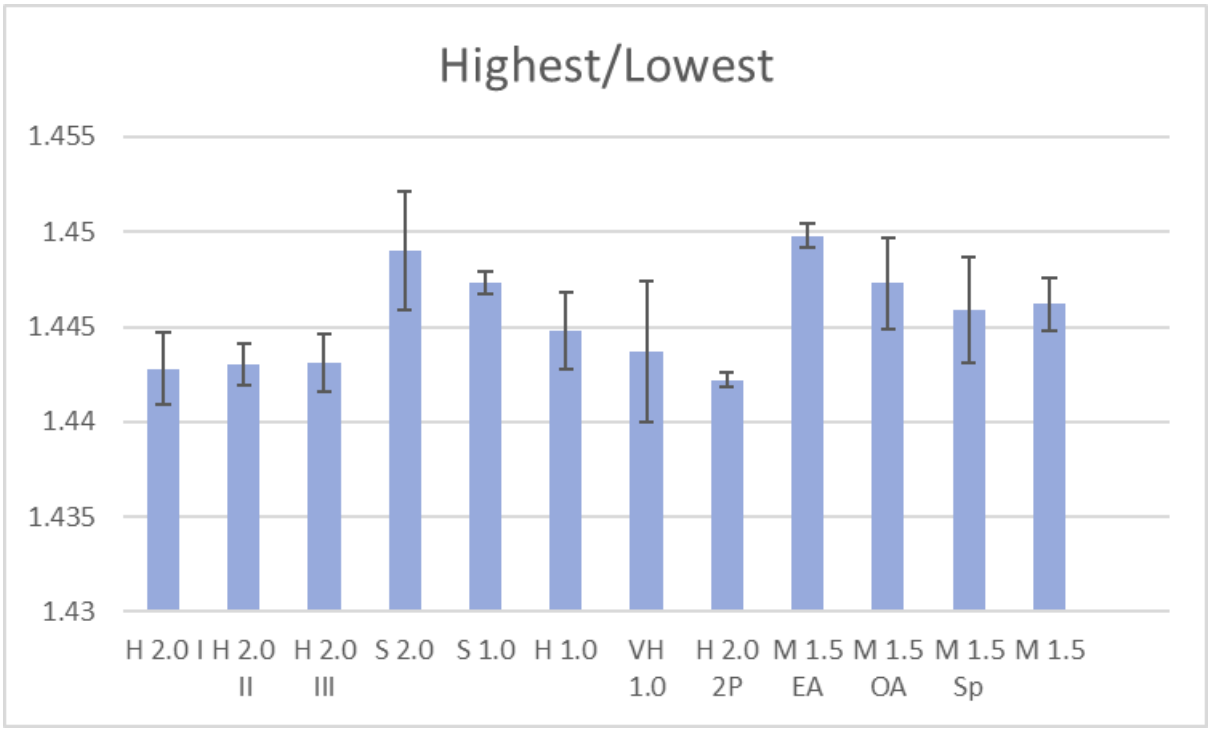

Figure 20, The ratio of the inserts

5. Discussion

5.1 Powder Characterisation

5.1.1 Correlation between compaction properties and PEG

The goal of the measurement was to find the insert with the most significant ratio, which indicates the biggest height difference between the lowest and highest points of the inserts and the greatest compaction properties. A correlation could be distinguished while comparing the PEG hardness for each powder with the ratio of the inserts. With reduced PEG hardness, the ratio of the inserts increased.

As shown in Table 7, both VH 1.0 and M 1.5 EA stick out from the pattern. It can be seen that M 1.5 EA, which has the biggest ratio, has a medium PEG hardness and does not follow the trend. What also stands out from the pattern is powder VH 1.0, which has the hardest PEG hardness but does not have the lowest ratio. VH 1.0 contains 1 wt% PEG compared to the powders with a smaller ratio with 2 wt% PEG added. This indicates that a lower weight percentage of PEG is correlated with greater compaction properties of the powders when looking at the harder PEG. This can be seen when analyzing powder H 1.0, which has a bigger ratio than VH 1.0, which is considered reasonable if one refers to the discovered correlation. This theory cannot be applied to the inserts with soft PEG as we could see that S 2.0 had a higher ratio than S 1.0.

It is distinguished in Table 8 that M 1.5 EA and M 1.5 OA were the two powders that had the highest ratio when analyzing the medium PEG hardness. M 1.5 EA was the powder with the best result in the ratio measurements, followed by the two powders with the soft PEG. In conclusion, the acid positively impacted the powder’s compaction properties.

5.1.2 Discussion of the test results

When analyzing Table 2, it is possible to discern a trend where the powders with the lowest measured weight, S 1.0 and H 1.0, also had the longest flow time. This is reasonable since these powders have the lowest gravitational force pulling the particles down through the hole, resulting in a longer time for these particles to flow through the hole. By instead comparing them to the powders with high density and weight, M 1.5 EA and M 1.5 OA, it is possible to discern that it does not correspond entirely to the pattern regarding that with a reduced weight of the powder, the flow time is longer.

For the angle of repose, it is difficult to see any trend in Figure 13 as the angle varies quite a bit even between powders with similar composition, as the three H 2.0. It is still interesting to note that for 1wt % of PEG, a more soft PEG is linked with a bigger angle. However, it is important to note that the standard deviation is around 6 % on average which is quite high, so the result needs to be considered carefully. M 1.5 Sp in particular has a high deviation.

When analyzing the results from Tap Density, the powders M 1.5 EA and M 1.5 OA stood out from the others with the highest density at both 0 and 3000 taps. This result raises the question of whether the acid content of these powders is what favors them in the test, by reducing the friction between the

particles and so allowing a better packing. Furthermore, the test also showed that the powders with hard and 2.0% PEG had higher densities than the powders with a lower hardness of PEG. This could mean that lower hardness causes more friction between particles. The precision of this measure is also very high, with less than 1% of uncertainty in general.

For the Hausner ratio, a low ratio means less difference between apparent and tap density. In Figure 15, the powders M 1.5 x all have a very similar ratio, which implies that their respective specificity was irrelevant on this test. As S 1.0 has a higher ratio, it can be theorized that a higher hardness and/or a higher concentration of PEG decreases the Hausner ratio. It can additionally mean that the PEG increases the apparent density or reduces the tap density. Both could be argued as PEG has a lower density than cemented carbide and hence, a higher concentration will decrease the overall density. However, a higher hardness could mean less friction and thus the particles could pack better from the beginning and exhibit a higher apparent density. The accuracy has less than 1 % of error.

Figure 7 and Table 4 show a link between the weight percentages and hardness of PEG and the particle size distribution. The harder and higher the percentage by weight, the lower the dispersion and the bigger the diameter. The concentration seems to have even more impact than the hardness seeing that the diameter values for S 2.0 and VH 1.0 are similar. The powder with the largest dispersion was S 1.0 with an *n* value of 6.05. Interestingly, H 1.0 and VH 1.0 had relatively high *n* values of 2.91 and 2.42, respectively. This indicates that the percentage content of PEG impacts the particle size distribution.

Three different parameters were computed in Table 5 concerning the shape of the particles. The aspect ratio had the most variation between the powder and the bigger deviation, showing that the particle's shapes were relatively similar in each powder. By looking at the shape on the size of the particles all powder shows an increase of the aspect ratio, as seen in Figure 11 and the convexity with the size but a decrease in sphericity (Figure 12). Indeed, comparing the size and aspect ratio, it can be seen that a lower median size corresponds to a lower aspect ratio. Interestingly, even inside one powder, the aspect ratio varies a lot more than the convexity, which varies more than the sphericity. Additionally, the values show that the particles are generally quite convex. At the same time, they are a bit less spherical and their aspect ratio varies between quite spherical and not really, which gives particles a shape around an ovoid.

Figure 16 shows the powder's flowability from the rheometer tests. The figure shows that the powders with the greatest resistance to the blade were S 1.0, S 2.0, M 1.5 SP, M 1.5 EA and M 1.5 OA. All powders with medium PEG follow the same trend with the exception of M 1.5 Sp, which increases faster when the speed of the blade decreases. Additionally, all powder with hard PEG followed the same curve, with H 1.0 as the exception which was just below M 1.5. S 1.0 and S 2.0 had the highest resistance with a maximum value between 2000-2500 mJ of total energy, while the other powders were below 1600 mJ. This indicates that the soft PEG generated a greater resistance than the harder PEGs due to a higher friction between the powder particles.

The shear tests of the rheometer are presented in Graph 17. In the graph, it is clear that all powders follow the same curve. The exception is powder S 1.0 which has a slightly higher value than the other powders but follows a similar curve. It was interesting to see that this was the first test with a similar value for almost all the powders. This indicates that PEG's different weight percentages and hardness do not affect the powder's shear strength. S 1.0 which was the exception has shown a tendency to differ from the other powders on all tests and had either the highest or lowest test value. This powder has the lowest density, softest and lowest weight percentage of PEG. The powder's low density could

be linked to its unique test performance. The FF and cohesion show an inverse trend, which is logic. If the flowability is good, so high, the cohesion will be low, showing that particles can easily move on each other. However, no clear link can be seen regarding the composition of the powder. A reason for this can be that this test is extremely sensitive to any impurity or agglomeration in the sample.

5.1.3 Correlation between compressibility and powder tests

When examining Table 2 the hall flow time versus the highest and lowest ratios, no clear trend is distinguished. However, when analyzing the calculated density, it is possible to see a trend when looking at powders M1.5 EA and M 1.5 OA. It can be distinguished that these powders have the same density, which is high compared to the other powders. In the same way, the two powders with soft PEG hardness, have lower density. One could say that they stand out against the remaining powders by breaking the increasing ratio and density trend. The trend is not straightforward but it is possible to discern that the S 2.0 and S 1.0 stand out in that they both have the lowest density but are still between the powder M 1.5 EA and the highest density with the largest ratio and M 1.5 OA which has the fourth highest ratio but has the same density as M 1.5 EA. What this generates for information with these tests is that it is possible to see a correlation between the density of the powder and the compaction properties but integration with one or a few other factors.

Regarding the angle of repose, it was difficult to discern a correlation between the highest and lowest ratios. According to the theory, the angle of repose is the steepest angle a powder can be piled on a flat surface without collapsing and the powder starting to flow. What is also known is that the angle of repose is lower for spherical particles, which in turn generates a good flow. By studying Table 4, it is possible to discern that powder S 1.0 is the powder with the highest angle of repose and the powder that tends to have the most spherical particles compared to the other powders. This is quite interesting since, according to the theory, this powder is supposed to have the least spherical particles as this generates good flow properties and, thus a lower angle of repose. As previously mentioned, only a small amount of a large powder batch was used, which means that the amount used in the particle size distribution test may have had more spherical particles than the portion of powder used in the angle of repose test. The test was carried out over different time periods where the powder can may have been shaken when subjected to movement. This is one reason the result may have turned out the way it did, but other aspects, such as the powder composition and the moisture content, should also be considered. With increased moisture content, the flow of the powder decreases, which can impact the result.

When examining Table 2 the powder with the lowest angle of repose, H 2.0 III, it is possible to discern from the comparison of sphericity in Table 4 that the powder is relatively similar to the rest of the powders. However, when examining whether the powder is more spherical, the powder tends to have fewer spherical particles than the others. Again, the results are inconsistent with the theory that powders with spherical particles have a low angle of repose. However, it is not sufficient to conclude specifically with this explanation without other aspects, such as moisture content and composition of the powder. Further, a pattern is distinguished when comparing the hall flow time and the angle of repose. With an increasing angle of repose, the hall flow time increases except for a few powders that differ from the pattern. This correlation is probably connected to flowability.

According to theory, a tap density test with a batch of spherical particles generates a high value of tap density. In contrast, irregular particles result in a lower value of tap density. To compare the results, the Hausner ratio is suitable to see the difference between the apparent and tapped densities. By

studying Table 6, it is possible to distinguish that the powders with medium PEG hardness all have a relatively high Hauser ratio. However, when analyzing the powders with soft PEG hardness, it is seen that S 2.0 has a small Hausner in contrast to S 1.0, which has the largest Hausner ratio compared to all twelve powders. The sphericity of S 1.0 in Table 4 shows that this powder has a high sphericity, which generates a higher tap density according to theory. By comparing the aspect ratio and density it can be seen that a lower aspect ratio is linked with a lower density and better compaction for all powders except the ones containing acid. Thus, the result in this particular case agrees with the theory. Regarding the results for the tap density measurements of both M 1.5 EA and OA, we can see that they have the highest apparent and tapped density. This is probably due to the density of the acid itself. In the Hall flow test, it is also possible to see that they have a lower time per gram.

Then looking at the result from the Particle Size Distribution a connection was observed with the measurements of the inserts. The powders containing the hard PEG had the lowest performance in the measurements of the inserts and the lowest distribution of particles in the PSD test (n value). They also have a smaller median diameter, mostly linked with a second peak in the small particles. In Figure 9, it can be seen that the PSD graph for powder M 1.5 EA gave the best measurement ratio. The graph shows two peaks indicating two different particle sizes in the powder. One reason for this connection may be that the smaller powder particles have the opportunity to fill gaps in the structure between the larger particles and can then create a more complicated geometry. A link can additionally be seen with the aspect ratio, higher-performing powder tends to have a lower value of aspect ratio, meaning that they tend to differ from a sphere and have a slightly more elongated shape. This result can be linked with a lower apparent density, due to the elongated shape, making the pressing process easier. These results mean that Particle Size Distribution might be able to be used as a method to use when investigating the compaction properties of powders. However, it is important to point out that H 1.0 was the powder with the second largest *n* value and has a rank of 7 on the measurement of inserts. This aspect is important to keep in mind when using the method.

Then looking at Figure 16 of the rheometer results on the flowability of the powder, a potential link with the ratio of the inserts could be seen. The figure shows that the powders with the greatest resistance to the blade were S 1.0, S 2.0, M 1.5 SP, M 1.5 EA and M 1.5 OA, which are all the powders with the best ratio in the measurements. The ones with the lower resistance are all the hard and very hard ones, which are also the ones with the lower ratio. The result indicates that the flowability of the powder is connected to its compaction properties. For the rheometer's tests on the shear strength of the powders, no clear link could be made to the measurements. As mentioned earlier, results indicate that PEG’s different weight percentages and hardness do not affect the powder's shear strength.

5.2 Ethical aspects

Exposure to cobalt can cause cancer and other health problems [5]. Today around 75% of the world's cobalt supply is mined in the Democratic Republic of the Congo (D.R.C). The cobalt mines use child labor and the workers work under slave-like conditions without protective equipment. Cobalt is used in producing smartphones, computers, and electric vehicles which have increased demand for the material. In Congo, the world's largest share of cobalt is mined at the expense of its population's health [23].

65-75 % of the cobalt Sandvik Coromant uses recycled material in their production [24]. Sandvik has certificates that their suppliers have to fulfill. They need to be able to show that they are following the laws and deliver material that can be traced to its origin. This means that Sandvik does not contribute

to the unfair treatment of people in D.R.C but also recycles a large part of its cobalt and thus makes a smaller footprint on the environment.

5.3 Sources of Errors

The main source of error is due to the definition of powder itself. A powder is a collection of particles that interact with each other. As each particle is different, each interaction will be slightly different. This makes it very complicated and not really representative to calcule a unique value as a result for any test, as any sample of the powder will be fundamentally different.

Something that should be considered is that only a small part of the large batch of powder has been used. This can lead to particle size variations, affecting many different aspects of the result. The flow rate, density, particle packing ratio, and compaction properties are all aspects that may be affected by this. In between the tests the powder's bottles were moved which could lead to granular convection, giving bigger particles on the tops. As the powder for the tests were poured or scooped by hand, even if it was done in a way not to take only the top it is possible that sizes were not totally representative.

The human reaction while measuring the time should be considered regarding hall flow. Furthermore, the powder quantities were measured by hand and can therefore vary and should be considered. We noted that the first test of each powder was always the fastest and had the lightest weight. These can indicate that powder particles may have been crushed during the process, larger powder masses could fit in the container, and the weight increased. This may have affected the result and the speed of the powder.

When doing the angle of repose the powders that had a high flowability fell easily from the plate when spun. This affected the angle and decreased each time the plate was spun. The powder that fell off the plate stuck under its foot, making it harder to spin. The harder it was to spin the plate, the easier it was to shake it and then make more powder fall off it. The angle of repose measurement equipment was not leveled correctly resulting in the cone of powder not being centered in the middle of the plate. Powder, therefore, ran down the plate on one side resulting in a lower angle than the other sides of the cone.

Regarding tap density measurement, it was difficult to distinguish an exact value when reading the volume from the measuring glass. The powder does not spread straight and horizontally, it rather differs in peaks and valleys, making it difficult to read the exact volume. The readings are something that can affect the result.

It is important to note that most tests were done in open air. Even with the controlled atmosphere of the lab, it is possible that the humidity and temperature influenced the results, creating agglomerate or changing the surface properties of the particles.

6. Conclusions

Based on the results and the discussion, the following conclusions were made:

- With a decreased hardness of the pressing agent, the compaction properties of the metal powder increase.
- A lower weight percentage of PEG improved the compaction properties when looking at harder PEG.
- Increased variation in particle size and smaller median diameter, generate greater compaction properties.
- There is a link between high resistance to a blade and good compaction properties in a powder.
- The powder with better compaction properties has a smaller aspect ratio.
- No clear correlation between the compaction properties and the angle of repose could be discerned, nor between the compaction properties and the hall flow.

7. Future Work

When looking at the medium PEG powders, the ones with acid added to them were the best-performing ones in ratio. For future studies, it would be interesting to investigate how adding Oleic acid and Erucic acid to the powders with soft peg would affect their compaction properties.

Due to time constraints, a Wall Friction Test was not performed. The test uses the Rheometer to measure the sliding resistance between the powder and the surface of the process equipment [19]. These measurements could have created an understanding of the powder's behavior during the pressing process and would be an interesting aspect of future research.

Furthermore, using another method to measure the inserts could be relevant to get an even more precise result. In the measurement of the inserts, a micrometer was used. This tool was not the most accurate and it was difficult to determine which point on the insert was the lowest. In future research, it may be relevant to use a digital measurement tool.

8. Acknowledgment

Firstly, we would like to thank our supervisors Christopher Hulme and Greta Lindwall from the Department of Material Science and Engineering at KTH. Your support and help with this project have been a great help throughout the process. We are very grateful for the time you were able to spend helping us with questions and testing the powders.

We would also like to thank our supervisors Hjalmar Staf, and Daniel Fredriksson
at the R&D department at Sandvik Coromant . Your expertise and support throughout this project have been of incredible help. Thank you for your time and that you provided us with this opportunity.

Finally, thank you to our examiner, Professor Anders Eliasson at the Unit of material science and Engineering at KTH for your support and guidance throughout this project.

Stockholm, May 2023
Emma Hjortzberg-Nordlund, Linnéa Lundemo Mattsson & Maeva Anfossi

9. References

[1] Chai Ren and Z.Zak Fang, “Methods for improving ductility of tungsten - A review,” *Science Direct,* [Online] Available: https://www.sciencedirect.com/science/article/pii/S0263436818300659 (accessed 2023-03-29)

[2] “Cutting tool materials”, *Sandvik Coromant.* [Online] Available: https://www.sandvik.coromant.com/en-gb/knowledge/materials/cutting-tool-materials.(accessed 2022-04-23)

[3] “Tungsten Carbide Cobalt (WC-Co, Cemented Carbide) Nanoparticles – Properties, Applications", *Azo Nano,* Jul. 18, 2013. [Online] Available: https://www.azonano.com/article.aspx?ArticleID=3358 (accessed 2023-02-05)

[4] “Tungsten Carbide Cobalt”, *Nano Partikel,* [Online] Available: https://nanopartikel.info/en/knowledge/materials/tungsten-carbide-cobalt/ (accessed 2023-02-05)

[5] J.M. Hogberg, “Ny forskning visar: Exponering av kobolt inom hårdmetallindustrin ger negativa hälsoeffekter,” *Nordiska Projekt,* Nov. 16, 2020. [Online] Available: https://www.nordiskaprojekt.se/2020/11/16/ny-forskning-visar-exponering-av-kobolt-inom-hardmetallindustrin-ger-negativa-halsoeffekter/ (accessed 2023-02-05)

[6] “The 3 Main Forming Agents in Production of WC and Their Usage,” *Meet you Carbie,* May. 22, 2019. [Online] Available: https://www.meetyoucarbide.com/the-3-main-forming-agents-in-production-of-wc-and-their-usage/?msclkid=b3ae5566cf8d11ecb32f730a7942fe86 (accessed 2023-02-05)

[7] PubChem. « Erucic Acid ». [Online] Available: https://pubchem.ncbi.nlm.nih.gov/compound/5281116.(accessed 2023-05-09)

[8] PubChem. « Oleic Acid ». [Online] Available: https://pubchem.ncbi.nlm.nih.gov/compound/445639.(accessed 2023-05-09)

[9] R. M. German, *Powder Metallurgy and Particulate Materials Processing*. 105 College Road East: Metal Powder Industries Federation, 2005. (accessed 2023-02-10)

[10] T.A. Bell, “Solids flowability measurement and interpretation in industry”, *Handbook of Powder Technology,* Volume 10, A. Levy, H. Kalman, Elsevier B.V., 2001, page 3-13 [Online] Available: https://www.sciencedirect.com/science/article/abs/pii/S0167378501800026 (accessed 2023-05-29)

[11] X. Gan, G. Fei, J. Wang, Z. Wang, M. Lavorgna, H. Xia, “Powder quality and electrical conductivity of selective laser sintered polymer composite components,” *Structure and Properties of Additive Manufactured Polymer Components*, Part 2, Elsevier Ltd., 2020. [Ebook] Available: https://www.sciencedirect.com/science/article/pii/B9780128195352000065 (accessed 2023-02-23)

[12] “Powder Flow Properties,” *Granu Tools,* Jul. 30, 2020. [Online] Available: https://www.granutools.com/en/news/59_powder-flow-properties (accessed 2023-02-25)

[13] “QICPIC,” *Sympatec*, [Online] Available: https://www.sympatec.com/en/particle-measurement/sensors/dynamic-image-analysis/qicpic/ (accessed 2023-04-01)

[14] K. A. Rosentrater, R. Bucklin, *Storage of Cereal Grains and Their Products,* 5th ed., Ames, IA: Elsevier Inc., 2022, ch. 6, pp. 135-178. [Ebook] Available: https://www-sciencedirect-com.focus.lib.kth.se/book/9780128127582/storage-of-cereal-grains-and-their-products#book-description (accessed 2023-02-05)

[15] T. F. Teferre, *Handbook of Farm, Dairy and Food Machinery Engineering*, 3th ed., Delmar, New York: Elsevier Inc., 2019, ch. 3, pp. 45-89. [Ebook] Available: https://www.sciencedirect.com/book/9780128148037/handbook-of-farm-dairy-and-food-machinery-engineering (accessed 2023-03-15)

[16] G. E. Amidon, P. J. Mayer, D. M. Mudie, “Particle, Powder, and Compact Characterization”, *Developing Solid Oral Dosage Forms,* 2nd ed., Y. Qiu, Y. Chen, G. G. Z. Zhang, L. Yu, R. V. Mantri, Ed., New Brunswick, NJ: Elsevier Inc., 2017, ch. 10, pp 271-293. [Ebook] Available: https://www-sciencedirect-com.focus.lib.kth.se/science/article/pii/B9780128024478000108 (accessed 2023-02-22)

[17] K. S. Narasimhan, “ Powder Characterization,” *Encyclopedia of Materials: Science and Technology,* K.H. Jürgen Buschow, Ed.: Elsevier Ltd., 2001, pp. 7781-7788. [Ebook] Available: https://www.sciencedirect.com/science/article/pii/B0080431526014005 (accessed 2023-02-22)

[18] “FT4 Powder Rheometer”, *Micromeritics,* Sep. 29, 2020. [Online] Available: https://www.micromeritics.com/ft4-powder-rheometer/ (accessed 2023-02-23)

[19] “Shear testing;” *Freeman Technology*, [Online] Available: https://www.freemantech.co.uk/powder-testing/ft4-powder-rheometer-powder-flow-tester/shear-testing (accessed 2023-04-26)

[20] “Particle Shape Analysis,” *Sympatec*, [Online] Available: https://www.sympatec.com/en/particle-measurement/glossary/particle-shape/ (accessed 2023-04-01)

[21] “Propagation of Error”, *Chemistry LibreTexts*,[online], Okt. 2, 2013. Available: https://chem.libretexts.org/Bookshelves/Analytical_Chemistry/Supplemental_Modules_(Analytical_Chemistry)/Quantifying_Nature/Significant_Digits/Propagation_of_Error. (accessed 2023-04-24)

[22] s. Divya, G.N.K. Ganesh, “Characterization of Powder Flowability Using FT4 – Powder Rheometer”, Journal of Pharmaceutical Sciences and Research, Vol 11, 2019, [Online] Available: https://www.proquest.com/openview/6e477c3a59eb8ca07c57bf2416b34d97/1?pq-origsite=gscholar&cbl=54977 (accessed 2023-04-25)

[23] T. Gross, “How 'modern-day slavery' in the Congo powers the rechargeable battery economy”, *National Public Radio,* [Online], Feb. 1, 2023. Available: https://www.npr.org/sections/goatsandsoda/2023/02/01/1152893248/red-cobalt-congo-drc-mining-siddharth-kara (accessed 2023-04-20)

[24] “Praktiska frågor om vår återvinningstjänst”, *Sandvik Coromant,* [Online], Available:

https://www.sandvik.coromant.com/sv-se/faq-carbide-recycling (accessed 2023-04-25)

Appendix: Test values

Summary of all values from the tests

Name	Ratio	HF(g/ml)	HF (s)	AOR (°)	HF s/g	mean aspect ratio	median aspect ratio	Hausner ratio	density 0 tapp	density 3000 tapps	D50 (µm)	n	mean convexity	FF	Cohesion kPa	flowability 10mm/s
M 1.5 EA	1.4498	3.82	41.96	28.44	0.4392	0.8	0.82	1.1903	3.718	4.425	54.55	1.92	0.91	10	0.311	1297
S 2.0	1.449	3.36	40.35	27.78	0.4809	0.8	0.82	1.1331	3.356	3.803	52.69	2.19	0.91	15.20	0.18	2095
S 1.0	1.4473	3.27	45.38	33.00	0.5545	0.75	0.75	1.225	3.215	3.939	17.11	6.05	0.89	8.82	0.31	2452
M 1.5 OA	1.4473	3.82	39.67	25.33	0.4158	0.8	0.82	1.1886	3.69	4.386	55.46	2	0.91	14.1	0.208	1330
M 1.5	1.4462	3.83	40.83	29.33	0.4850	0.78	0.80	1.1858	3.333	3.953	40.25	2.8	0.91	12.00	0.24	1259
M 1.5 SP	1.4459	3.4	41.46	28.39	0.4878	0.79	0.81	1.1804	3.322	3.922	48.89	2.57	0.91	32	0.0841	1515
H 1.0	1.4448	3.34	42.79	30.44	0.5117	0.78	0.79	1.193	3.3	3.937	40.63	2.91	0.9	11.8	0.234	1188
VH 1.0	1.4437	3.39	41	27.67	0.4844	0.79	0.81	1.1541	3.333	3.847	51	2.42	0.91	21.6	0.125	635
H 2.0 III	1.4431	3.38	39.08	25.00	0.4631	0.84	0.88	1.1042	3.367	3.718	79.4	1.51	0.93	27.4	0.103	675
H 2.0 II	1.443	3.53	40.33	26.67	0.4856	0.95	0.95	1.1289	3.46	3.906	108.75	1.17	0.95	53.6	0.0498	716
H 2.0 I	1.4428	3.48	42.19	30.00	0.4574	0.89	0.92	1.1474	3.472	3.984	99.67	1.19	0.94	19.10	0.16	656
H 2.0 2P	1.4422	3.51	38.77	26.39	0.4422	0.85	0.89	1.1674	3.413	3.984	81.6	1.33	0.93	12.90	0.22	644

TRITA – 2023:148